8-2010

THE EFFECTS OF PHYSICAL FACTORS ON THE ADSORPTION OF SYNTHETIC ORGANIC COMPOUNDS BY ACTIVATED CARBONS AND ACTIVATED CARBON FIBERS

Hatice Kose
Clemson University, selcenkose@gmail.com

THE EFFECTS OF PHYSICAL FACTORS ON THE ADSORPTION OF SYNTHETIC ORGANIC COMPOUNDS BY ACTIVATED CARBONS AND ACTIVATED CARBON FIBERS

A Thesis
Presented to
the Graduate School of
Clemson University

In Partial Fulfillment
of the Requirements for the Degree
Master of Science
Environmental Engineering and Earth Sciences

---

by
Hatice Selcen Kose
August 2010

Accepted by:
Dr. Tanju Karanfil, Committee Chair
Dr. Cindy Lee
Dr. David Freedman

ABSTRACT

Activated carbons (ACs) and activated carbon fibers (ACFs) have been extensively used for the removal of synthetic organic compounds (SOCs) that have been found to be toxic, carcinogenic, mutagenic or teratogenic. Adsorption of these compounds on ACs and ACFs are controlled by both physical factors and chemical interactions, which depend on the characteristics of the adsorbent (surface area, pore size distribution (PSD), and surface chemistry), the nature of the adsorbate (molecular weight and size, functional groups, polarity, solubility), and the condition of the background solution (pH, temperature, presence of competitive solutes, ionic strength). Since there are several mechanisms that can affect the adsorption, it is important to understand the role of these individual factors responsible for the adsorption of a given combination of adsorbate and adsorbent under certain background conditions.

The main objective of this study was to conduct a systematic experimental investigation to understand the effects of physical factors on the adsorption of SOCs by different porous carbonaceous adsorbents. Three ACFs, with different activation levels, and three granular activated carbons (GACs) produced from two different base materials were obtained, characterized and used in the experiments. The single solute adsorption isotherms of the selected carbons were performed for benzene (BNZ), biphenyl (BP), phenanthrene (PHE) and 2-hydroxybiphenyl (2HB).

First, the role of carbon structure on the adsorption was examined and the accessible pore size regions for BNZ, BP and PHE were determined. It was found that adsorption of the selected SOCs was higher for ACFs than those of GACs due to the

higher microporosity (more than 75%) and higher specific surface areas of ACFs. Both PSD and pore volume in pores less than 1 nm were important for the adsorption of BNZ, whereas accessible pore size regions for BP and PHE were determined to be approximately 1 - 2 nm. While adsorption of BNZ was found to be correlated with both surface areas and pore volumes, adsorption of BP and PHE was only related to the surface areas of carbons. These relationships showed that there was no restriction for BNZ molecules to access the pores of the carbons, whereas size exclusion effects were observed for BP and PHE adsorption.

Second, the effects of the molecular structure, dimension and configuration of the selected SOCs were investigated. The adsorption uptake increased with decreasing molecular dimension of each compound, and the uptake was in the order of BNZ > BP > PHE for the six heat-treated carbons. The nonplanar BP had an advantage over the planar PHE, since it was more flexible, and thus, able to access deeper regions of the pores than the rigid PHE. It was observed that BP had higher adsorption capacities as expressed on mass-basis than those of 2HB at the same concentration levels. This was attributed to the different solubilities of these SOCs since they were very similar in molecular size and configuration. On the other hand, after their concentrations were normalized with solubility, at the same reduced concentration levels, the adsorption capacities of 2HB were higher than those of BP due to the π-π electron-donor-acceptor interactions that resulted from the hydroxyl group in the 2HB.

Finally, to examine the role of surface oxidation, BP and 2HB adsorption isotherms on the heat-treated and oxidized ACFs were performed. The nitrogen

adsorption data demonstrated that heat treatment increased the microporous surface areas by 2 to 13% compared to the oxidation of the ACF samples. Comparing the oxidized to the heat-treated ACFs, oxidized ACFs had higher oxygen and nitrogen contents and water vapor uptakes, which confirmed that they were more hydrophilic, than the heat-treated ACFs. Adsorption isotherm results demonstrated that the heat-treated ACFs had higher adsorption capacities than the oxidized ACFs, demonstrating that surface polarity had an important role in the adsorption of aromatic compounds.

DEDICATION

I would like to dedicate this thesis to my family.

ACKNOWLEDGMENTS

First and foremost, I would like to thank my advisor, Dr. Tanju Karanfil, for his guidance, patience and support during my graduate study, and my committee members, Dr. Cindy Lee and Dr. David Freedman, for their insight and expertise.

I will always remember all the wonderful people with whom I have shared my life in Clemson, especially those are in Dr. Karanfil's research group. Many special thanks to Dr. Shujuan Zhang, my honorary advisor, for her continuous help, expertise and technical support with the carbon preparation and characterization works. I am also thankful to Dr. Sehnaz Sule Kaplan Bekaroglu for being generous to share her knowledge and lab skills with me all the time.

I would like to acknowledge the Republic of Turkey, Ministry of National Education for funding my education in US. This work was also partly supported by a research grant from National Science Foundation (CBET 0730694).

Finally, I am thankful to my parents and my sister for their unconditional love and understanding. Without their support I would have never come this far. I am also grateful to my best friends, Sezin Kilincci, Meric Selbes and Devin Shippey, for their love and encouragements.

TABLE OF CONTENTS

Page

Table of Contents (Continued)

Page

LIST OF TABLES

LIST OF FIGURES

List of Figures (Continued)

Figure Page

LIST OF ABBREVIATIONS

AC	Activated Carbon
ACF	Activated Carbon Fiber
BC	Black Carbon
BET	Brunauer-Emmett-Teller equation
BJH	Barret-Joyner-Halenda
BNZ	Benzene
BP	Biphenyl
DDW	Distilled and Deionized Water
DFT	Density Functional Theory
EDA	Electron Donor Acceptor
FM	Freundlich Model
GAC	Granular Activated Carbon
HPLC	High Performance Liquid Chromatography
LFM	Langmuir-Freundlich Model
LM	Langmuir Model
MTBE	Methyl Tertiary Butyl Ether
PAC	Powdered Activated Carbon
PCB	Polychlorinated Biphenyl
pH	$-\log\{H^+\}$
pH_{PZC}	pH of point of zero charge
PHE	Phenanthrene
pKa	-log{Ka}
PMM	Polanyi-Manes Models
RMSE	Residual Root Mean Square Error
PSD	Pore Size Distribution
SOC	Synthetic Organic Chemical
STM	Scanning Tunneling Microscopy
TCB	1,2,4-trichlorobenzene
TCE	Trichloroethylene
USEPA	United States Environmental Protection Agency
2HB	2-hydoxybiphenyl

CHAPTER ONE

INTRODUCTION

A large number of synthetic organic compounds (SOCs) have been produced for the purpose of industrial and domestic uses for many years. Most of them have been found to be toxic, carcinogenic, mutagenic or teratogenic. These compounds may enter the aquatic environment from atmospheric sources, industrial and municipal effluent, and agricultural runoff. Since the existence of these compounds in water sources has been detected, the Clean Water Act and its amendments have been promulgated by the United States Environmental Protection Agency (USEPA) to protect public health and natural resources [USEPA, 1995]. The Safe Drinking Water Act and its amendments followed the Clean Water Act in order to protect the public from exposure to some of these undesirable and harmful chemicals. Currently, nearly one hundred SOCs are classified as priority pollutants and regulated by the USEPA [2009].

The Safe Drinking Water Act Amendments of 1986 cited activated carbon (AC) adsorption as one of the "Best Available Technologies" to remove SOCs from aqueous environments [Le Cloirec et al., 1997; Karanfil and Kilduff, 1999; Moreno-Castilla, 2004; USEPA, 2009]. In order to develop more effective ways for the removal of adsorbates by AC adsorption and to predict their control, fate and transport in the environment, it is critical to gain a fundamental understanding of the chemical interactions and physical factors involved in the adsorption of SOCs by ACs. In general, AC has a well developed porous structure and a large internal surface area (e.g., 800-1000 m^2/g). It consists of 87 to 97% carbon and such elements as oxygen, hydrogen,

sulfur and nitrogen as well as some inorganic components either originating from the raw materials or chemicals used in its production. A wide variety of materials can be used for producing AC, such as wood, coal, bituminous coal, rubber, almond shells, oil-palm stones, polymers, phenolic resins, and rice husks [Choma and Jaroniec, 2006].

Recently, activated carbon fibers (ACFs) have gained increased popularity due to their unique pore structure properties that provide a higher adsorption capacity. ACFs exhibit narrower and more homogeneous pore size distributions (PSDs) than the heterogeneous pore structure of ACs. They are usually highly microporous (pores less than 2 nm are dominant in the pore structure), and these micropores are directly accessible from the external surface of the fiber. Therefore, without the additional diffusion resistance of macropores observed for ACs, molecules with small molecular sizes reach adsorption sites through micropores. Due to high microporosity, ACFs are selective for the adsorption of low-molecular-weight compounds [Kaneko et al., 1989; Le Cloirec et al., 1997; Moreno-Castilla, 2004].

Adsorption of SOCs on ACs and ACFs are affected by both physical and chemical factors such as the characteristics of the adsorbent (surface area, PSD, surface chemistry) and the adsorbate (molecular weight, size, functional groups present, polarity, hydrophobicity, solubility), and the background solution conditions (pH, temperature, presence of competitive solutes, ionic strength) [Radovic et al., 1997; Li et al., 2002; Dabrowski et al., 2005; Villacanas et al., 2006; Guo et al., 2008].

The accessible pore volume to a molecule of a given size is determined by PSD. In order to calculate the distribution of pore sizes, it is necessary to develop a model for

pore filling that relates the pore width to the condensation pressure [Lastoskie et al., 1993a]. Pore filling is the main physical adsorption mechanism in small micropores because the overlapping of pore wall potentials results in stronger binding of the adsorbate, or enhanced adsorption. In the case of some organic molecules of a large size, molecular sieve effects may occur either because the pore width is narrower than the dimensions of the adsorbate molecules or because the shape of the pores does not allow the molecules of the adsorbate to penetrate into the micropores. Therefore, even though there are multiple contact points between the adsorbate and adsorbent, larger molecules do not experience this enhanced adsorption phenomenon. In addition, slit-shaped micropores formed by the spaces between the carbon layer planes are not accessible to molecules of spherical geometry that have a diameter larger than the pore width [Pelekani and Snoeyink, 2000; Menendez-Diaz and Martin-Gullon, 2006].

Water cluster formation around the polar sites of carbonaceous adsorbent surfaces is also one of the important factors affecting the adsorption of SOCs. AC-water interactions are related to the surface polarity of the carbon. Hydrophilic surface sites, which may include both acidic (e.g., oxygen-containing) and basic (e.g., nitrogen-containing) functionalities as well as inorganic (e.g., metal) species, cause the surface polarity. The functional groups existing on ACF surfaces are adsorption sites of water molecules and they are more likely to be found at the edge of carbon sheets [Kaneko et al., 1989; Salame and Bandosz, 1999]. The adsorbed water clusters may block carbon pores and reduce sorption capacity of hydrophobic compounds. Several studies have documented that water clusters can prevent SOC molecules access to the microporous

surface of carbonaceous adsorbents [Karanfil and Kilduff, 1999; Karanfil and Dastgheib, 2004]. Since the majority of the AC surface area for adsorption is located within the micropores, water cluster formation is particularly important for adsorption of SOCs at low concentrations.

Both molecular conformation and dimensions of an adsorbate affect the adsorption. The molecular dimension of a SOC with respect to the PSD of an adsorbent is important since it determines the accessible surface area or pore volume for adsorption. Depending on the molecular dimensions of a target SOC, there is an optimum carbon pore size region that maximizes the uptake of the SOC. The studies on the effects of molecular conformation of adsorbate in the adsorption process are relatively limited. A recent study performed by Guo et al. [2008] showed that planar molecules accessed and packed in the slit-shape pores more efficiently as compared to nonplanar molecules. Moreover, nonplanar molecular conformation weakened the interactions between adsorbate molecules and carbon surfaces. Results of the study by Guo et al. [2008] confirmed that molecular conformation of SOCs has an important effect on adsorption.

Besides molecular dimension and conformation, solubility of an adsorbate also has significant effects on the adsorption. Compounds that have low solubilities prefer accumulating on the carbon surface rather than dissolving in water. As a result, the adsorption of an organic compound by AC or ACF increases with decreasing solubility in the solvent [Dowaidar et al., 2007].

To date, many studies have been performed to understand and examine the chemical interactions in the adsorption of organic compounds. However, there has been

limited research about the role of physical factors in the adsorption process. **The main objective of this study was to systematically investigate the effects of physical factors (surface area and pore structure of adsorbent, and molecular dimension and molecular configuration of adsorbate) on the adsorption of SOCs by different porous carbonaceous adsorbents.**

This study was a portion of a project funded by National Science Foundation that has examined and compared adsorption of SOCs by a range of carbonaceous adsorbents (AC, ACF, Single Walled Nanotubes, Multi Walled Nanotubes, and Graphite). Although not presented and discussed in this thesis, the results were also used to compare adsorption behavior of a selected number of SOCs with several carbonaceous adsorbents [Zhang et al., 2010].

CHAPTER TWO

LITERATURE REVIEW

The objective of this chapter is to provide a literature review on the preparations, structures and applications of ACs and ACFs, the interactions controlling the adsorption of SOCs, and the influencing factors in SOC – carbon interactions.

2.1 Activated Carbons and Activated Carbon Fibers

ACs are carbonaceous materials which have been efficiently used in several pollution control systems due to their high adsorption capacity. They can be found in the forms of granular activated carbon (GAC) and powdered activated carbon (PAC). They are typically produced from relatively heterogeneous base materials such as bituminous coal, charcoal, lignite, coconut shells, peat or wood, which are materials with high carbon content and low inorganic components [Dabrowski et al., 2005]. While the particles of GACs have irregular shapes with commercially available sizes ranging from 0.5 to 2.5 mm, PACs are a pulverized form of GACs with a size predominantly less than 0.15 mm [Karanfil, 2006].

ACFs are prepared from homogeneous polymeric materials such as polyacrylonitrile, cellulose or phenolic resin [Li et al., 2002]. They provide a number of advantages over conventional GACs and PACs. ACFs are highly microporous (> 90% by pore volume), with micropores directly on the external surface of fibers having an average diameter from 5 to 21 Å (Figure 2.1). Due to the high microporosities, ACFs are selective for the adsorption of low-molecular-weight compounds [Kaneko et al., 1989;

Moreno-Castilla, 2004]. Their unique pore structure properties make them very effective in removing contaminants from liquid or air with adsorption rates and capacities higher than those of GACs and PACs. Initial adsorption rates are 2.5-10 times larger with fibers [Le Cloirec et al., 1997; Guo et al., 2008]. In addition, the higher carbon and lower ash contents of ACFs make them more hydrophobic than GACs and PACs [Kaneko et al., 1993]. Since ACFs are usually commercially available as fiber cloths, it is convenient to incorporate them into the existing treatment systems by immersion into tanks or pipes. However, the manufacturing cost is high [Shmidt et al., 1997], and the relatively high cost of ACF is currently a major barrier and prevents its widespread application in water and wastewater treatment. While the price of ACF can cost as much as $100 per pound, GAC is comparatively cheaper at only around $1 per pound [Economy's Group, 2003].

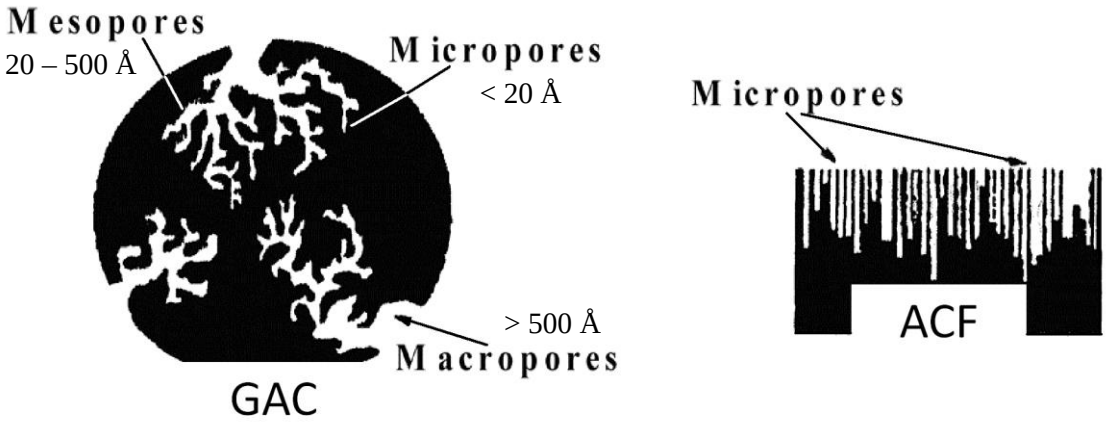

Figure 2.1 Schematic pore structures of GAC and ACF.

2.1.1 Preparation of Carbons

Solid carbonaceous based materials, which are non-graphitic, are used as precursors for the preparation of ACs. The precursor is transformed or 'activated' by means of medium to high temperature treatments. As a result, not only solid mass is removed but also pores are created where the removed mass was previously located. The precursor is very important for both the activation process and the final properties of a given carbon adsorbent [Menendez-Diaz and Martin-Gullon, 2006]. There are some criteria considered in the selection of the precursors [Dabrowski et al., 2005]:

- low inorganic matter content,
- ease of activation,
- availability and cost, and
- low degradation during storage.

The production methods can be classified into two categories:

(i) Thermal activation (or physical activation): Generally consists of two consecutive steps, thermal carbonization and activation. Thermal carbonization of the raw material is accomplished at medium or high temperatures and devolatilization takes place at this step. The aim of this is to produce a char rich in carbon. In the activation step, the remaining char is partially gasified with an oxidizing agent (mostly steam) in direct fired furnaces. If both steps are carried out simultaneously, the process is called direct activation [Menendez-Diaz and Martin-Gullon, 2006].

(ii) Chemical activation: The raw material is first impregnated by considerable amounts of a chemical agent such as phosphoric acid, zinc chloride, or alkaline hydroxides, and

then heated. After carbonization, the impregnated product must be washed to remove excess chemical agent [Menendez-Diaz and Martin-Gullon, 2006].

The precursors of ACF are polyacrylonitrile fibers, cellulose fibers, phenolic resin fibers or pitch fibers, and cloths or felts. The ACFs are produced, mainly, by the thermal activation of carbonized carbon fibers. They are first carbonized at a temperature of 800 - 1000 °C to remove noncarbonaceous components and to develop a limited pore volume, and then physically activated at 800 - 1100°C in an atmosphere of steam or CO_2 to increase pore surface area and volume [Brasquet and Le Cloirec, 1997; Le Cloirec et al., 1997]. Specific surface areas as high as 2500 m^2/g or higher may be obtained by this way. However, ACFs with specific surface area of 2000 m^2/g are usually the practical limit for most purposes because of the increased cost, reduced yield and decrease of textile properties, and ACFs with 1500 m^2/g surface areas are adequate for many applications [Hayes, 1985].

2.1.2 Structures of Carbons

The large surface area of an AC is almost only within the particles, and it is structurally considered to be made up of clusters (microcrystallites) that are rigidly interconnected, and each of them consists of a stack of graphitic planes [Snoeyink et al., 1969]. Graphite is a layered structure in which the graphene layers (single graphite plane) are formed by atoms of carbon bonded by σ- and π- bonds to another three neighboring carbon atoms (sp^2-based structure). The graphite planes tend to exhibit a parallel alignment which is maintained by dispersive and van der Waals forces (Figure 2.2).

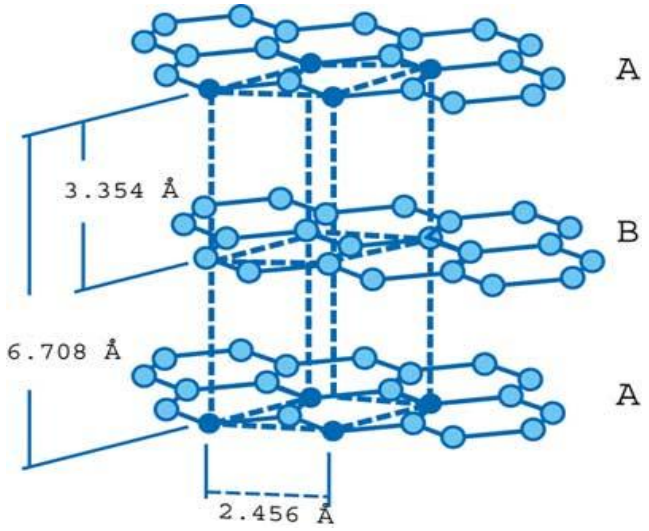

Figure 2.2 Structure of graphite crystal [Electronics Cooling, 2001].

A carbon adsorbent has a porous structure, which is perhaps the main physical property that characterizes an AC. Pore size of adsorbents are classified into four groups according to the International Union of Pure and Applied Chemistry recommendations: (1) Macropores with a pore width larger than 500 Å, (2) Mesopores with widths from 20 to 500 Å, (3) Secondary micropores with widths from 8 to 20 Å, and (4) Primary micropores with a pore width less than 8 Å [Lastoskie et al., 1993b; Pelekani and Snoeyink, 1999]. For example, coconut shell carbons are considered microporous because the majority of their total void volume is microporous, whereas wood-based carbons have a more even distribution of micro-, meso-, and macropores [Crittenden et al., 2005].

Various heteroatoms, such as oxygen, hydrogen, nitrogen, phosphorus and sulfur, are on the surface of ACs. These heteroatoms mainly originated from the starting material, and they are chemically connected to the carbon surface during the synthesis

process, forming carbon-heteroatom structures [Karanfil and Kilduff, 1999; Considine et. al., 2001]. Some ACs also contain variable amounts of inorganic matter (ash content) depending on the nature of the raw material used as precursor.

Besides surface groups and inorganic ash, the heterogeneous surface of AC is also characterized by the carbon basal planes as an adsorption zone. The majority of the adsorption sites for liquid organics are on the basal planes, which forms more than 90% of the carbon surface [Franz et al., 2000]. The basal planes of the microcrystallites exposed within the micropore fissures during activation constitute the intraparticle surface of the AC. The edges of the graphitic planes include the sides of the microcrystallites. These microcrystallites are estimated to be a stack of 5 - 15 layers of graphitic planes with a diameter or height of about 2 - 5 nm [Wolff, 1959; Snoeyink and Weber, 1967].

The pores of ACFs are relatively small and uniform. The nature of the precursor and the graphitic character of the ACFs provide narrow and uniform pore size distributions (PSDs). In order to examine both the surface and interior structure of phenolic resin-based ACFs, Daley et al. [1996] used scanning tunneling microscopy (STM). Elongated and ellipsoidal micropores and mesopores were observed at the fiber surface and the size of the surface mesopores increased with increasing degree of activation. Randomly distributed and homogeneous ellipsoidal micropores and small mesopores were present over the fiber cross-section [Daley et al., 1996; Pelekani and Snoeyink, 2000]. Once activation of ACFs is initiated, the gasification continues to the neighboring edge sites along the same graphene sheet creating pores that are confined

within two graphene sheets. As a result, the pores are approximately 7 - 10 Å in size and elongated within two graphene sheets. Also, the PSD and the pore size in the ACFs can be modified by adding a catalyst before activation [Freeman et al., 1989].

2.1.3 Properties and Application of Carbons

Highly developed internal surface areas and porosities of ACs and ACFs allow them to adsorb large amounts and various types of chemicals from gases or liquids, and thus, making them highly preferential in many applications [Kyotani, 2000]. Applications include the production of high purity water in electronics manufacturing, hospitals and medical laboratories; industrial wastewater treatment; municipal water filtration; solvent recovery such as gasoline vapor recovery in gasoline loading facilities; chlorofluorocarbon recovery in foam blowing; separation of gas mixtures such as removal of hydrogen sulfide from natural gas; removal of sulfur dioxide and nitrous oxides from flue gases; removal of mercury vapor from air, hydrogen, methane and other gases; air conditioning systems; cigarette filters; military uses (gas masks and respirators, defence clothing etc.); automotive evaporation control systems; and in liquid-phase applications either for odor, color or taste removal from a solution or concentration or recovery of a solute from solution, and so forth. [Shmidt et al., 1997; Choma and Jaroniec, 2006; Przepiorski, 2006].

The physicochemical characteristics of PACs, GACs and ACFs make them useful in specific applications. For example, PACs have faster adsorption rates than GACs; however, PACs compact under flow, resulting in a strong flow resistance. Even though ACF has a high adsorption rate, its adsorption capacity of heavy metals is low. The

possibility of preparation of ACFs as woven cloth and non-woven mats provides new applications in small purification systems for city water and also as a refrigerator deodorizer in private houses [Inagaki and Tascon, 2006]. Both ACs and ACFs are used in heterogeneous catalysis because they can act as catalysts for many reactions and as supports for immobilization of different catalysts. They are excellent supports due to their resistance to acidic and basic media, high thermal stability in an oxygen free atmosphere, high surface area and tailorable PSD [Choma and Jaroniec, 2006].

2.2 Adsorption of SOCs

Three types of interactions control the adsorption of low-molecular-weight SOCs on ACs and ACFs. These are (i) SOC-carbon interaction which is controlled by the physicochemical properties of the carbons, the molecular structures of the SOCs, and the solution chemistry, (ii) SOC-water interaction which is related to the chemical compatibility between SOC molecules and water, and (iii) carbon-water interaction which depends on the polarity of the carbon. These interactions are discussed in detail in the following sections.

2.2.1 SOC - Carbon Interactions

The interactions between adsorbents and adsorbates are controlled by the physicochemical properties of the AC, the molecular structure of the SOC, and the solution chemistry. Physical, chemical and electrostatic interactions have been identified as the three types of interactions between the carbon surface and the adsorbates

[Summers and Roberts 1988a, 1988b; Weber et al., 1991; Radovic et al., 1997; Karanfil and Kilduff, 1999; Moreno-Castilla, 2004].

During physical adsorption, which is also called as physisorption, the electrons maintain their association with the original nuclei, whereas during chemical adsorption (i.e., chemisorption) there is a transfer and/or sharing of electrons between the adsorbate molecules and the carbon surface. Electrostatic interaction occurs between adsorbate ions and charged functional groups on the carbon surface [Weber and Van Vliet, 1980]. The relative strength of these interactions depends on the combination of adsorbate and adsorbent, as well as the background solution.

2.2.1.1 Physisorption

There are four types of physical interactions: (1) London dispersive energy, (2) Debye energy, (3) Keesom energy, and (4) Coulombic (dipole-dipole) [Weber et al., 1991]. Forces associated with interactions between the dipole moments of sorbate and sorbent molecules commonly underlie physical sorption processes. Dipole moments are caused by charge separation within a molecule and can be either permanent or induced. If molecules have a permanent dipole moment, they are referred to as polar molecules. Interactions between polar molecules or between polar molecules and nonpolar molecules represent one class of "physical" sorption.

The physisorption of aromatics on the ACs mainly occurs through dispersive interactions between the aromatic molecules and the carbon basal planes. These dispersive interactions are basically in the form of van der Waals interactions [Franz et al., 2000].

2.2.1.2 Chemisorption

Chemisorption occurs when there is a significant affinity between the solute and the carbon surface and as a result the molecular orbitals overlap in the respective phases. The bonds that form between solute molecules and surface chemical groups show all of the characteristics of true chemical bonds, and they are characterized by relatively large heats of sorption. The reactions may include a considerable amount of activation energies and be favored by high temperatures [Weber et al., 1991].

Chemisorption includes different kind of interactions such as electron donor-acceptor interaction between the carbonyl oxygen on the carbon surface (donor) and the electron deficient aromatic ring of the solute (acceptor), and the hydrogen-bonding between the oxygen-containing surface functional groups (carboxylic and hydroxyl groups) and similar functional groups of the solute [Weber and Van Vliet, 1980].

2.2.1.3 Electrostatic Interactions

Electrostatic interactions occur between ionized SOC and the charged functional groups on the carbon surface. Weak organic acids and bases dissociate in solution. The degree of this dissociation depends on the magnitude of the difference between the pK_a of the SOC molecules and the pH of the solution. The surface of the carbon has a net positive or negative charge depending upon the pH of the solution and the pH of the point of zero charge (pH_{PZC}) of the carbon. When the pH of the media is higher than the pH_{PZC}, the surface charge is predominantly negative. In this case, electrostatic interactions are more important than the dispersive interactions. On the other hand, the surface charge will be predominantly positive if the pH is lower than the pH_{PZC}. This suggests that

dispersion forces control the adsorption process [Radovic et al., 1997]. Overall, there will be either electrostatic attraction or repulsion between the carbon surface and the ionizable SOC depending on the pH of the media, pK_a of the SOC molecules, and pH_{PZC} of the carbon.

2.2.2 SOC - Water Interactions

The chemical compatibility between SOC molecules and water is the main factor that determines SOC - water interactions [Karanfil and Kilduff, 1999]. The hydrophobic characteristic of a SOC is the driving force for the molecule to escape to the interfaces between solvent and adsorbent surface because hydrophobic compounds are energetically favorable to accumulate at a soil-water interface rather than to remain in water. This phenomenon is called 'Solvent Motivated Sorption' [Weber et al., 1991; Karanfil and Dastgheib, 2004]. The solubility of an organic compound decreases as the chain length of organic subunits increases, and consequently the adsorption increases [Weber, 1972]. This is valid only in the absence of the size exclusion effect, which limits the access of adsorbate molecules to the deeper region of carbon pores.

The polarity of SOC molecules results from the difference in the electronegativities among the various atoms, which causes an unequal distribution of electron density. While nonpolar compounds are retained due to dispersive forces, the adsorption of polar compounds includes specific interactions via oxygen, nitrogen and other species on the surface [Ania et al., 2008]. The solubility of a compound decreases with increasing difference between its polarity and the polarity of the solvent. Therefore,

adsorption of a SOC by AC increases as its solubility in the solvent decreases [Dowaidar et al., 2007].

In order to eliminate the differences in hydrophobicity among the adsorbates, adsorption can be normalized with respect to the solubility. These normalized isotherms reflect the capacity for the adsorbent surface [Moreno-Castilla, 2004; Carrott et al., 2005].

2.2.3 Carbon - Water Interactions

Carbon - water interactions depend on the polarity of the carbon surface. The presence of hydrophilic centers renders the carbon surface polar, and enhances the interaction with polar liquids such as water [Ania et al., 2008]. When water comes to the carbon surface, it adsorbs on the hydrophilic, polar oxygen groups located at the entrance of the carbon pores [Franz et al., 2000]. This enhanced interaction leads to formation of water clusters on the carbon surface, which reduces the accessibility and affinity of organic molecules to the inner pores where the majority of the carbon surface area is located. This is especially important for adsorption of SOCs at low concentrations, since water clusters clog the micropores which are the primary adsorption sites for SOC molecules [Karanfil and Dastgheib, 2004].

2.3 Influencing Factors in SOC - Carbon Interactions

Despite the fact that there have been many studies on the effects of chemical interactions in the adsorption process, limited studies have been performed on the role of physical factors, such as the effects of pore structure and molecular conformation of the

compounds. Therefore, besides the chemical interactions involved in the adsorption of SOCs, a fundamental understanding of the physical factors is critical to predict the fate and transport of SOCs in the environment.

2.3.1 Pore Structure of Carbons

2.3.1.1 Pore Size Distribution of Carbons

The ACs (PACs and GACs) typically exhibit a heterogeneous pore structure where micropores, mesopores and macropores are present, whereas ACFs exhibit more uniform PSDs [Li et al., 2002]. As one of the most important properties which influence the adsorption process, the PSD determines the fraction of the total pore volume that can be accessed by an adsorbate of a given size [Pelekani and Snoeyink, 1999]. This influence occurs in two ways: (i) if pores are too small, size exclusion limits the adsorption of contaminants of a given size and shape; and (ii) adsorption strength increases with decreasing pore size. As pore size decreases, contact points between the adsorbate and the adsorbent surface increase, and adsorption potentials between opposing pore walls begin to overlap [Li et al., 2002; Karanfil and Dastgheib, 2004; Bandosz, 2006]. When opposing pore walls are separated by little more than the diameter of an adsorbed molecule, the adsorption forces in micropores increase. Most of the adsorption of organics takes place within micropores, since they comprise the largest part of the internal surface area of carbon [Pelekani and Snoeyink, 1999]. The adsorption mechanism in micropores is considered to be mainly pore filling due to overlapping of pore wall potentials which results in stronger binding of the adsorbate. Even if there are

multiple contact points between the adsorbate and adsorbent, larger molecules do not experience this adsorption phenomenon because they are not able to access the micropores. In this case, adsorption selectivity or molecular sieve ability can develop in primary micropores. As the pore size increases, the selectivity for the primary micropores decreases and the selectivity may increase for most of the secondary micropores [Pelekani and Snoeyink, 2000]. For example, Le Cloirec et al. [1997] studied the selectivity of ACF by performing two adsorption experiments, one with a mixture of phenol and humic substances and one with phenol alone. Similar isotherm curves were obtained for both experiments, which showed humic substances were not being removed by ACF. The ACF exhibited selectivity for the phenol (low molecular weight molecules) compared to humic substances (macromolecules) due to its high microporosity.

Kasaoka et al. [1989] found that when micropores were present, adsorption occurred only when the average micropore diameter increased to about 1.7 times the second widest dimension of the adsorbate's molecule. Li et al. [2002] observed that even small changes in the micropore size distribution of an adsorbent (e.g., 7 - 11 Å widths in ACF10 versus 9 - 13 Å widths in ACF15 and ACF20) altered the effectiveness of an adsorbent for a given micropollutant. Similarly, the study of Karanfil and Dastgheib [2004] demonstrated that the adsorption of trichloroethylene (TCE) by ACF and GAC increased as the pore volume in the micropore region of < 10 Å increased. While the optimum pore size region for TCE adsorption is pores < 10 Å, especially the 5 - 8 Å region, optimum adsorption pore size region for atrazine was determined to be 8 - 20 Å by Guo et al. [2007].

2.3.1.2 Pore Geometry of Carbons

Both the base material and activation conditions have an effect on the pore structure. Pore structure is important because it affects the accessibilities of the adsorbate molecules to the pores and subsequently their packing in the pores, such that slit-shaped micropores are not accessible to molecules of spherical geometry that have a diameter larger than the pore width [Menendez-Diaz and Martin-Gullon, 2006].

The measured PSDs depend on the shape of the model pores used in the analyses. There are three commonly used model pores: slit-shaped, square and rectangular. Slit-shaped pores represent the simplest and the least complicated description of the internal structure when compared to square and rectangular model pores. However, slit-shaped pores are simplified representation of the void spaces within the adsorbent, because they do not include ‘‘corners’’ that are likely to be present when two or more planes of carbon meet. On the other hand, in square and rectangular model pores, the corners show the same behavior as small pores in the analysis based on slit-shaped model pores. This leads to PSDs based on square and rectangular model pores to be flatter and moved to larger pore sizes compared to those determined using slit-shaped pores [Davies and Seaton, 1998].

Pore structure shows significant differences between GACs and ACFs. Using STM analysis, both Stoeckli et al. [1995] and Paredes et al. [2003] demonstrated that GACs mainly contained two-dimensional slit pores and three-dimensional cross-linked spaces resulting from the deflection of carbon hexagons from the planes of graphene

layers. On the other hand, ellipsoidal micropores were observed in ACFs which range in size from several angstroms to as large as 2.5 nm in width by Daley et al. [1996].

Li et al. [2002] investigated the effect of pore structure on the adsorption of TCE and methyl tertiary butyl ether (MTBE). They found that when the pores of the ACFs were elliptical, the flat TCE molecule was able to access pores with a smaller dimension along the minor axis than the MTBE molecule, which has a tetrahedron structure. In a recent study performed by Guo et al. [2008], it was demonstrated that SOC molecules could access and fill more efficiently the slit-shaped pores than ellipsoidal pores. While the access of SOC molecules to the slit-shaped pores was mainly restricted by one dimension (i.e., the thickness of the adsorbate molecules), their access to the ellipsoidal pores was restricted by two dimensions (i.e., both width and thickness of adsorbate molecules).

2.3.2 Surface Chemistry of Carbons

Surface chemistry is related to functional groups found on the carbonaceous adsorbent. These surface functional groups are important to the adsorption process because they influence the adsorption properties and reactivities of the carbons. Several techniques can be used to modify the surface chemistry of a carbon. Heat treatment, oxidation, amination, and impregnation with various inorganic compounds are some of the modification methods [Karanfil and Kilduff, 1999]. Beside surface reactivity, these methods may also change structural and chemical properties of the carbon including the extent of both electrostatic and dispersive interactions [Radovic et al., 1997; Karanfil and Kilduff, 1999]. For instance, oxidation of the carbon lowers pH_{PZC} as well as reduces the

dispersive adsorption potential by decreasing the π-electron density in the graphene layers [Radovic et al., 1997].

Functional groups make the carbon surface either basic or acidic. While oxygen-containing surface functional groups are related to acidity, nitrogen-containing functional groups increase the basicity of the carbon surface [Mangun et al., 2001]. With increasing oxygen-containing functional groups on the carbon surface, acidity and polarity of the surface increase [Karanfil and Kilduff, 1999]. AC can be modified by heat-treatment in order to remove the oxygen containing surface groups. It has been reported that the adsorption affinity of phenolic compounds increases with increasing basicity (hydrophobicity) of the carbon surface [Menendez et al., 1996; Stavropoulos et al., 2007]. Specifically, it has been demonstrated by several researchers that oxidized surfaces exhibit reduced uptakes of SOCs [Coughlin et al., 1968; Karanfil and Kilduff, 1999; Li et al., 2002; Garcia et al., 2004]. Water adsorption is the mechanism behind the decrease in the adsorption uptake with surface oxygenation. Water adsorbs through hydrogen-bonding and causes built up of water clusters around hydrophilic oxygen groups [Franz et al., 2000].

Karanfil and Kilduff [1999] investigated the role of the GAC surface chemistry on the adsorption of TCE and 1,2,4-trichlorobenzene (TCB). The results indicated that TCE and TCB uptake by both coal based and wood-based carbon decreased with oxidation of the carbons due to the increasing surface acidity or polarity. After strong acidic functional groups were selectively removed from the surface by heat treatment following the surface oxidation, the adsorption capacities of TCE and TCB were increased. Performing

adsorption experiments by using phenanthrene, Garcia et al. [2004] observed that the surface chemistry of the activated carbons had an important role. The adsorption capacity was higher for ACs with a low concentration of surface oxygen groups than for ACs with a high concentration of surface oxygen groups. Similarly, Coughlin and co-workers [1968] found that both phenol and nitrobenzene sorption increased with reduction and decreased with oxidation of the AC surface. In the study of Kaneko et al. [1989], the adsorption capacities of untreated ACF and H_2-gas-treated ACF were tested. Their findings showed that both the nonpolar molecule (e.g., benzene) adsorption and the polar molecule (e.g., nitrobenzene) adsorption were higher on the highly hydrophobic H_2-gas-treated ACF than on the untreated ACF.

2.3.3 Molecular Properties of SOCs

The physicochemical properties of an adsorbate have important effects on the adsorption as much as those of adsorbents because the capacity and rate of adsorption also depend on the nature of the adsorbed molecule [Ania et al., 2008]. While the molecular dimension and molecular conformation controls the accessibility to the pores, the solubility determines the hydrophobic interactions. It has been shown that the adsorption rate constant decreases with increasing molecular size of the adsorbate [Pignatello and Xing, 1996].

2.3.3.1 Size and Configuration of SOCs

The interaction efficiency between a hydrophobic adsorbate and a carbonaceous adsorbent is generally affected by two factors; (i) dispersive interactions between sorbate

and sorbent electron systems and (ii) the sorbate-sorbent separation distance (steric effects). Cornelissen et al. [2004] investigated the importance of black carbon (BC) sorption for planar and nonplanar molecules. They observed that among the two factors mentioned above, steric hindrance was the one that rendered the strong, specific BC sorption sites less accessible for nonplanar 2,2′-dichlorobiphenyl (2,2′-PCB). This probably indicated that nonplanar 2,2′-PCB was too "thick" for fitting into the majority of narrow BC nanopores, whereas the thickness of the planar compounds was below the average BC nanopore size.

Jonker and co-workers [2000, 2001 and 2002] conducted a series of adsorption experiments for planar and nonplanar PCBs. Their findings showed that coplanar PCBs exhibited stronger sorption on the soot and soot-like materials as compared to nonplanar congeners. The reason was attributed to the ability of the planar compounds to approach the flat sorption surface very closely, creating favorable π-cloud overlap and, thus, enhancing sorption in narrow pores.

Guo et al. [2008] systematically investigated the effects of molecular conformation and molecular dimension on the adsorption of three different SOCs: biphenyl, 2-chlorobiphenyl and phenanthrene. The uptake of SOCs by the heat-treated ACF10 in water followed the order of biphenyl > phenanthrene ≈ 2-chlorobiphenyl. Among these SOCs, 2-chlorobiphenyl had the lowest uptake due to its nonplanar conformation. Even though the molecular configuration of phenanthrene and biphenyl were planar in the adsorbed state, biphenyl seemed to adjust its molecular conformation

and filled the pores more effectively than phenanthrene. Biphenyl had a higher accessibility to the pore because of its smaller width.

2.3.3.2 Hydrophobicity and Polarity of SOCs

Several studies have demonstrated that adsorption of a SOC by ACs and ACFs increases with decreasing solubility and/or increasing hydrophobicity in the solvent due to the development of driving forces for SOC molecules to escape to interfaces. In other words, adsorption of a hydrophilic compound is energetically less favored than adsorption of a hydrophobic one, for which solute/solvent interactions are weaker [Kaneko et al., 1989; Li et al., 2002; Karanfil and Dastgheib, 2004; Derylo-Marczewska et al., 2004; Villacanas et al., 2006; Dowaidar et al., 2007].

Kaneko et al. [1989] investigated the adsorption of benzene derivatives in water. For both untreated ACF and H_2-treated ACF, the amount of adsorbed organics increased with decreasing solubility in water (Table 2.1), which was benzene > nitrobenzene > benzoic acid > phenol. Similarly, Derylo-Marczewska et al. [2004] and Villacanas et al. [2006] also conducted adsorption experiments for benzene derivatives and found consistent results. Derylo-Marczewska et al. [2004] performed experiments with nitrobenzene, 4-nitrophenol, 4-chlorophenol, phenol. While nitrobenzene was adsorbed very strongly, 4-nitrophenol and 4-chlorophenol adsorption was weaker, and phenol adsorption was the weakest. Likewise, Villacanas et al. [2006] investigated the adsorption behavior of nitrobenzene, aniline and phenol. For the same equilibrium concentration, the amount adsorbed decreased from nitrobenzene >> aniline > phenol with increasing solubility. Li et al. [2002] evaluated TCE (relatively hydrophobic) and MTBE (relatively

hydrophilic) adsorption in water for assessment of adsorbate polarity effect. Regardless of the pore structure or surface chemistry, adsorbents always showed larger adsorptive affinities for TCE than for MTBE. The solubilities of above-mentioned SOCs are summarized in Table 2.1.

Table 2.1 Water solubilities of the SOCs at 25°C.

Compounds	**Solubility** (g/L)
Benzene[a]	1.77
TCE[b]	1.2
Nitrobenzene[c]	2.1
Benzoic acid[a]	3.4
4-nitrophenol[a]	11
4-chlorophenol[a]	27
Aniline[c]	33.8
MTBE[b]	50
Phenol[c]	86.6

[a] CRC [1990-1991]; [b] Li et al. [2002]; [c] Villacanas et al. [2006].

In summary, it has been shown that physical factors affect the adsorption of SOCs by ACs and ACFs since they control the accessibility of the adsorbate molecules to the pores, and the subsequent packing of the adsorbate molecules in the pores. However, there is limited information about the quantitative relationship between physical factors and adsorption affinities. This study will provide this relationship as well as a further understanding of the effects of physical factors.

CHAPTER THREE

RESEARCH OBJECTIVES

The overall objective of this study was to conduct a systematic experimental investigation to examine the effects of physical factors on the adsorption of synthetic organic compounds (SOCs) by porous carbonaceous adsorbents. To accomplish this objective, three specific objectives were developed and experimental plans were designed and conducted for each of them.

The first objective of the study was to examine the role of carbonaceous adsorbent physical characteristics (i.e., surface area, pore size distribution) on SOC adsorption. Benzene (BNZ), phenanthrene (PHE) and biphenyl (BP) were used as adsorbates. The heat-treated forms of three activated carbon fibers (ACFs) and three granular activated carbons (GACs) were used in order to minimize any impact that might be caused by the presence of surface functional groups on the diffusion of adsorbate molecules into deeper pore regions. The size of adsorbent pores affects the adsorption of organic contaminants in two ways. First, adsorption strength increases with decreasing pore size. Second, size exclusion limits the adsorption of contaminants of a given size and shape if pores are smaller than the adsorbate [Li et al., 2002]. For this objective, the accessible pore size regions of porous carbonaceous sorbents to the SOCs and pore size distributions (PSDs) were determined, and the roles of adsorbent structure on the adsorption of SOCs were examined.

The second objective was to investigate the role of SOC physical characteristics (structure, dimension and configuration) on adsorption by ACs. For this objective, BNZ, PHE, BP and 2-hydroxybiphenyl (2HB) were selected as adsorbates. While BNZ, PHE and BP were used to examine the effects of molecular dimension and molecular configuration, BP and 2HB adsorptions were compared to understand the hydrophobicity effect and investigate any specific interactions. Both BNZ and PHE are planar molecules, whereas BP has nonplanar configuration in water and planar configuration in adsorbed state [Guo et al., 2008]. BNZ has the smallest molecular size and highest solubility as compared to BP and PHE. The heat-treated ACFs and GACs were used as adsorbents in this phase. The properties of both adsorbents and adsorbates selected for this study resulted in the carbon basal plane (i.e., graphene layer) as the main adsorption sites, especially at low concentrations or low degrees of surface coverage. Other interactions that affect the adsorption, such as specific interactions with surface groups, electrostatic interactions, dipole-dipole interactions were minimized by the surface treatment. Thus, the simplification of the adsorption system made it possible to examine the effects of molecular configurations of adsorbates with respect to the pore structure or topography of graphene layers of adsorbents. The heat-treated and oxidized ACFs were also used as adsorbents to examine adsorption of BP and 2HB and the effect of SOC hydrophobicity on adsorption. While BP and 2HB are very similar in terms of molecular configuration and molecular dimension, their solubilities, and consequently hydrophobicity, are quite different.

Finally, the last objective was to investigate the impact of the carbonaceous adsorbent surface oxidation (i.e., oxidized vs. heat-treated ACs) on SOC adsorption. Although the main impact of oxidation is to change the surface characteristics of carbons, it may also impact physical characteristics. Adsorption of BP and 2HB on both heat-treated and oxidized ACFs were performed and compared. Water adsorption isotherms and detailed characterization of the adsorbents were also obtained to interpret the experimental results.

CHAPTER FOUR

MATERIALS AND METHODS

4.1 Adsorbents

Nine different carbons (Table 4.1) prepared from different precursor materials and with different physical characteristics were used for this study. Three heat-treated granular activated carbons (GACs) [a coconut shell-based: OLC (Calgon Carbon Corporation); two coal-based: F400 (Calgon Carbon Corporation) and HD4000 (Norit Inc.)), and three heat-treated and three oxidized phenol formaldehyde-based activated carbon fibers (ACF10, ACF15 and ACF20 (American Kynol Inc.)] were used in this study. The carbons were prepared by Dr. Shujuan Zhang, a post doctoral research associate in Dr. Tanju Karanfil's laboratory, using the methods described in one of the previous studies of Dr. Karanfil's research group [Dastgheib et al., 2004]. Carbons were treated under hydrogen flow for 2 hours at 1173 K in a quartz reactor. The purpose of heat treatment was to remove most of the functional groups, and to decrease the acidity of the carbon surface [Puri, 1970; Considine et al., 2001]. Many studies have shown that the presence of oxygen-containing surface functionalities has a negative impact on the adsorption of synthetic organic compounds (SOCs) due to the formation of water clusters on the surface of the carbons [Li et al., 2002; Karanfil et al., 2006]. The heat-treated samples were labeled as ACF10-H_2, ACF15-H_2, ACF20-H_2, OLC-H_2, F400-H_2, and HD4000-H_2, where H_2 stands for the hydrogen treatment.

Adsorbent-water interactions were investigated by comparing three heat-treated ACFs with three oxidized ACFs. ACFs were oxidized by 4 M nitric acid for 1 h at 363 K in order to add surface functional groups. The increase in functional groups by the oxidation enhances the hydrophilic character of the carbon adsorbents, which is important for the purpose of this study [Corapcioglu and Huang, 1987; Considine et al., 2001; Dastgheib and Rockstraw, 2001]. The oxidized ACFs were labeled as ACF10-NO, ACF15-NO, and ACF20-NO.

Table 4.1 Summary of the adsorbents used in this study.

Adsorbent	Full name	Precursor	Company
ACF10-H_2	heat-treated activated carbon fiber ACF10*	phenol formaldehyde-based	American Kynol Inc.
ACF15-H_2	heat-treated activated carbon fiber ACF15	phenol formaldehyde-based	American Kynol Inc.
ACF20-H_2	heat-treated activated carbon fiber ACF20	phenol formaldehyde-based	American Kynol Inc.
ACF10-NO	oxidized activated carbon fiber ACF10	phenol formaldehyde-based	American Kynol Inc.
ACF15-NO	oxidized activated carbon fiber ACF15	phenol formaldehyde-based	American Kynol Inc.
ACF20-NO	oxidized activated carbon fiber ACF20	phenol formaldehyde-based	American Kynol Inc.
OLC-H_2	heat-treated granular activated carbon OLC	coconut shell-based	Calgon Carbon Corporation
F400-H_2	heat-treated granular activated carbon Filtrasorb 400	coal-based	Calgon Carbon Corporation
HD4000-H_2	heat-treated granular activated carbon Hydrodarco 4000	coal-based	Norit Inc.

* Brand names given by the companies.

4.2 Adsorbates

The SOCs selected for this study have different molecular configurations (planar and nonplanar) and electrochemical properties including both single/polycyclic and substituted/unsubstituted aromatic hydrocarbons. The four compounds are benzene (BNZ, planar, 99.8+%), phenanthrene (PHE, planar with three aromatic rings, 97+%), biphenyl (BP, nonplanar in water but planar in adsorbed state, 99.5+%), and 2-hydroxybiphenyl (2HB, nonplanar in both water and adsorbed state, with a strong hydrogen donating group at an *ortho* position, 99+%). Some of the properties of these SOCs are summarized in Table 4.2 and molecular structures are illustrated in Figure 4.1. Adsorption of BNZ, PHE and BP were compared for investigation of the pore structure and pore size distribution (PSD) effects because of their different molecular dimensions and molecular structures. In order to examine the hydrophobicity effect, adsorption of BP and 2HB were compared; because, they are very similar in terms of molecular configuration and molecular dimension, whereas their solubilities are quite different.

Table 4.2 Physicochemical properties of SOCs.

SOC	**Molecular Configuration**	**Molecular size**[a] (Å × Å × Å)	**MW**[b] (g/mol)	**Density** (g/cm^3)	**MV**[c] (cm^3/mol)	S_w[d] (mg/L)	log K_{ow}[e]
BNZ	Planar	7.4 × 6.7 × 3.4	78.11	0.879	88.86	1770	2.22 ± 0.15
PHE	Planar	11.7 × 8.0 × 3.4	178.23	1.063	167.67	1.1	4.68 ± 0.17
BP*	Nonplanar	11.8 × 6.8 × 4.7	154.21	0.992	155.45	6.1	3.98 ± 0.23
2HB	Nonplanar	11.8 × 7.8 × 5.4	170.21	1.213	140.32	700	2.94 ± 0.25

*Nonplanar in water, planar in adsorbed state; [a] Simulated with ACDLABS11.0 (ChemSketch and ACD/3D Viewer); [b] Molecular weight; [c] Molecular volume; [d] Water solubility at 25 °C obtained from the Material Safety Data Sheet of each compound; [e] Simulated with ACDLABS11.0 (ChemSketch and ACD/3D Viewer).

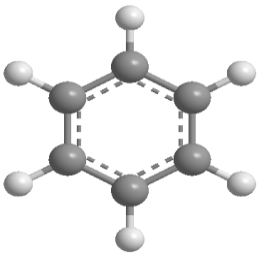

BNZ

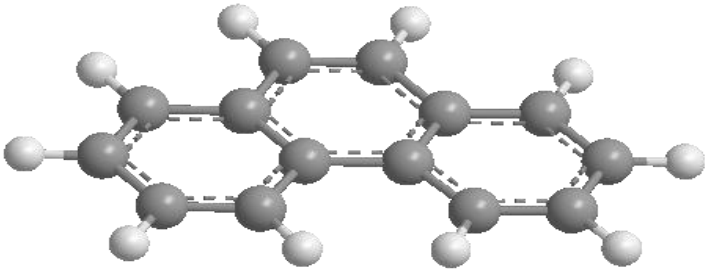

PHE

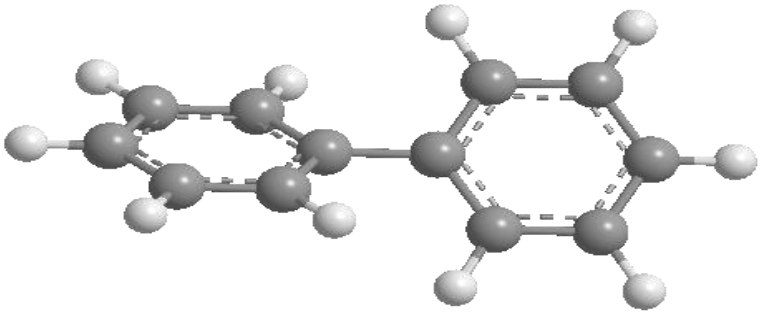

BP

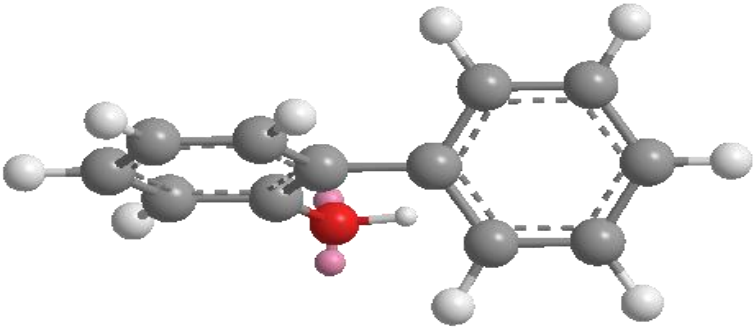

2HB

Figure 4.1 Molecular structures of SOCs (Simulated with ACDLABS 11.0).

4.3 Characterization of Adsorbents

The physicochemical properties of adsorbents were characterized by using various techniques: (i) Nitrogen adsorption for surface area and PSD (ASAP 2010 Physisorption/Chemisorption Analyzer and Micromeritics' Density Functional Theory (DFT) model); (ii) elemental analysis for the determination of carbon, hydrogen, nitrogen, sulfur, and oxygen (CHNSO elemental analyzer); (iii) water vapor adsorption (ASAP 2010 physisorption/chemisorptions analyzer); and (iv) the pH of the point of zero charge (pH_{PZC}). Carbon characterization was performed by Dr. Shujuan Zhang using the techniques described in Sections 4.3.1, 4.3.2, and 4.3.3.

4.3.1 Surface Area and Pore Size Distribution

Nitrogen gas adsorption isotherms, volumetrically obtained from a relative pressure range of 10^{-6} to 10^{0} at 77 K, were used to determine the surface area and PSD of the carbons. Surface areas of these carbons were calculated by the Brunauer-Emmett-Teller (BET) equation using the adsorption data within 0.01 to 0.1 relative pressure ranges. Micromeritics DFT software was used to determine the PSD. A graphite model with slit shape pore geometry was assumed in the PSD calculation. While the total pore volume was determined by using the adsorbed volume of the nitrogen near the saturation point ($P/P_o = 0.98$), the Dubinin-Redushkevich equation in the relative pressure range 10^{-5} to 10^{-1} was used to determine the micropore volume. The difference between total and the micropore volumes was designated as the total mesopore and macropore volume. Triplicate results of randomly selected samples were used to determine the

reproducibility of the data and the relative standard deviation of the BET surface area, micropore volume and the total pore volume was lower than 10%.

4.3.1.1 Brunauer-Emmett-Teller Model

Brunauer et al. [1938] generalized a form of the Langmuir isotherm by incorporating the concept of multilayer adsorption to formulate the BET model. This model is used to determine the surface area of a sample, and it is based on the assumption that the forces responsible for the binding energy in multimolecular layer adsorption are the same as those involved in the condensation of gases. The BET equation is obtained by equating the rate of condensation of the molecules onto an already adsorbed layer to the rate of evaporation from that layer and summing for an infinite number of layers. Rearranging that equation in a linear form results in the following BET equation [Webb and Orr, 1997]:

$$\frac{P}{V_a(P_0 - P)} = \frac{1}{V_m C} + \frac{C - 1}{V_m C}\left(\frac{P}{P_0}\right) \tag{4.1}$$

Where,

P_0: Saturation pressure of the adsorption gas.

V_a: Quantity of gas adsorbed at pressure P.

V_m: Quantity of gas adsorbed when the entire surface is covered with a monomolecular layer.

C: Constant.

The volume of the monolayer (V_m) can be obtained by plotting $P/(V_a(P_0-P))$ versus P/P_0, where $1/V_mC$ is the intercept and $(C-1)/V_mC$ is the slope of the linear plot. It is

possible to determine the surface area of the sample by knowing the volume of the monolayer adsorption and the area occupied by a single adsorbate molecule, such as 16.2 $Å^2$ for nitrogen, 21.0 $Å^2$ for krypton, 14.2 $Å^2$ for argon and 17.0 $Å^2$ for CO_2 [Webb and Orr, 1997].

4.3.2 pH_{PZC}

The pH_{PZC} was determined according to the method described in Karanfil and Dastgheib [2004]. Distilled and deionized water (DDW) was boiled to remove dissolved CO_2. The boiled DDW was used to prepare 0.1 M NaCl solutions with the pH in the range of 2 to 11 adjusted with either 0.5 N HCl or 0.5 N NaOH solutions. 75 mg of the carbon sample and 15 mL of the 0.1 M NaCl solutions with different pH values were added into 20 mL vials. On a table shaker at room temperature, the vials were shaken at 200 rpm. After 48 hours contact time, they were left on a bench to allow the carbons to settle. The final pH of the solution was measured using a pH meter (Metrohm/702 SM Titrino). The pH_{PZC} was determined as the pH of the NaCl solution which did not change after contacting the carbon samples. Duplicate runs were also performed for randomly selected samples and the reproducibility of the measurements was within ± 0.2 units.

4.3.3 Water Vapor Adsorption

Water vapor isotherms of the adsorbents used in this study were volumetrically obtained at 273 K by using the Micromeritics ASAP 2010 Physisorption/Chemisorption Analyzer. The experiments provided direct information about the surface hydrophilicity of the carbons. At the low relative pressure range (P/P_0 = 0.0 to 0.4) the water vapor

uptake is related to the extent of water cluster formation around the hydrophilic sites [Mowla et al., 2003; Karanfil and Dastgheib, 2004; Karanfil et al., 2006]. In order to remove the moisture and other adsorbed vapors/gases, approximately 50-100 mg of carbon sample was degassed for a period of 1 hour at 363 K and overnight at 473 K. The degassed samples were then transferred to the analysis port and adsorption data points were collected. Data were collected in the relative pressure range of 10^{-4} - 10^{0} (P/P_0).

4.4 Isotherm Experiments

Constant dose bottle point technique was used for the single solute isotherm experiments. Experiments were performed in 255 mL amber glass bottles with Teflon-lined screw caps. One mg of ACFs and GACs were equilibrated in solutions with different concentrations of BNZ, BP and 2HB, whereas 0.5 mg of carbons was equilibrated in solutions of PHE due to its low solubility. Concentrated stock solutions of each adsorbate were prepared in methanol. The bottles were first filled with DDW to nearly full, and then were spiked with predetermined volumes of stock adsorbate solutions. The bottles were then placed on a tumbler for one week at room temperature (21 ± 3°C). After the equilibration period, remaining liquid phase concentrations were analyzed using both UV-Vis spectrophotometer and a high performance liquid chromatography (HPLC). A 4.6 x 150 mm and 5-micron size HPLC column (Agilent / Zorbax Extend-C18 type) was used at a flow rate of 1 ml/min for analyses. The maximum absorption wavelength and isocratic elution proportion of each SOC are presented in Table 4.3. The bottles without any adsorbent were used as blanks to monitor the loss of adsorbates during the experiments, which was found to be negligible. All

experiments were performed at room temperature (21 ± 3°C). The experimental matrix of SOC adsorption on the ACFs and GACs is shown in Table 4.4.

Table 4.3 Analytical conditions for UV-Vis and HPLC for determination of SOCs.

	UV	**HPLC**		
SOCs	(nm)	Eluent DDW/MeOH[a] (%)	FL-λ_{ex}[b] (nm)	FL-λ_{em}[c] (nm)
BNZ	254	20/80	254	280
PHE	250	20/80	293	366
BP	248	20/80	260	315
2HB	245	40/60	290	340

[a] Volumetric proportions of DDW and methanol (v:v); [b] Fluorescence excitation wavelength;
[c] Fluorescence emission wavelength.

Table 4.4 Experimental matrix.

Adsorbates / **Adsorbents**	BNZ	PHE	BP	2HB
ACF10-H_2	3[a] [10][b]	3 [8]	3 [10]	3 [19]
ACF15-H_2	3 [10]	3 [8]	3 [10]	3 [10]
ACF20-H_2	3 [10]	3 [8]	3 [10]	3 [20]
ACF10-NO	NC	NC	3 [20]	3 [30]
ACF15-NO	NC	NC	3 [10]	3 [30]
ACF20-NO	NC	NC	3 [20]	3 [20]
OLC-H_2	3 [10]	3 [15]	3 [10]	NC
F400-H_2	3 [10]	3 [8]	3 [10]	NC
HD4000-H_2	3 [10]	3 [8]	3 [10]	NC

[a] Number of isotherms conducted; [b] Number of data points used for regression analyses; NC: Not conducted.

4.5 Data Analysis

Four isotherm models, Freundlich, Langmuir, Langmuir-Freundlich, and Polanyi-Manes models, were applied to the experimental data.

The Freundlich model is an empirical equation, and perhaps the most widely used nonlinear sorption model because it accurately describes much adsorption data for heterogeneous adsorbent surfaces. This model is expressed as:

$$q_e = K_F C_e^n \tag{5.2}$$

Where, q_e and C_e represent the solid-phase equilibrium concentration (mg/g) and the aqueous phase equilibrium concentration (μg/L or mg/L), respectively. While K_F is the Freundlich equilibrium affinity parameter ((mg/g)/C_e^n), n represents the exponential parameter related to the magnitude of the driving force for the adsorption and the distribution of adsorption site energies, and ranges between 0 and 1 [Weber, 1972]. A larger K_F value represents a larger adsorption affinity, whereas a larger n value indicates a more homogeneous surface of the adsorbent [Derylo-Marczewska et al. 1984; Carter et al. 1995; Pikaar et. al., 2006].

The Langmuir model has a theoretical basis and is perhaps conceptually the most straightforward non-linear isotherm model. The Langmuir equation often does not describe adsorption data by activated carbons as accurately as the Freundlich equation, probably because a homogeneous surface is assumed in the model. The Langmuir equation is

$$q_e = \frac{q_m b C_e}{1 + bC_e} \tag{5.3}$$

Where, q_m represents the maximum adsorption capacity and corresponds to the surface concentration at monolayer coverage, and b is related to the energy of adsorption and increases as the strength of the bond increases [Snoeyink and Summers, 1999].

The Langmuir-Freundlich model is a composite of the Langmuir and the Freundlich isotherms, and it is capable of modeling both heterogeneous and homogeneous surfaces. The equation has the following form:

$$q_e = \frac{q_m K_s C_e^n}{1 + K_s C_e^n} \tag{5.4}$$

Where, K_S [$(L/\mu g)^n$] is adsorption affinity coefficient, and n represents a nonlinear index [Sips, 1948].

The Polanyi adsorption potential theory was developed by several researchers including Manes and co-workers [Manes and Hofer, 1969; Chiou and Manes, 1973; Chiou and Manes, 1974]. The overall theory was later referred as the Polanyi-Manes model which is widely employed for adsorption surfaces with heterogeneous energy distribution:

$$q_e = q_m \times 10^{\left[a\left(\frac{\epsilon}{V_s}\right)^b\right]} \tag{5.5}$$

Where, a and b are fitting parameters and V_s is molar volume of solute. ϵ is the Polanyi adsorption potential and can be expressed as $\epsilon = RT \ln(C_s / C_e)$ [kJ/mol], where C_s is the water solubility of the adsorbate, R is the ideal gas constant and T is the absolute temperature.

CHAPTER FIVE

RESULTS AND DISCUSSION

The results obtained in this study will be presented in this chapter. First, characterization of the carbons will be provided in order to describe the differences and similarities among them, which will be followed by the discussion of the modeling of experimental data with different isotherm equations. Subsequently, the results of the adsorption experiments will be presented for each objective of the study.

5.1 Characteristics of Adsorbents

5.1.1 Pore Structure of Carbons

Pore structures and pore size distributions (PSDs) of the activated carbon fibers (ACFs) and granular activated carbons (GACs) were obtained from nitrogen adsorption isotherms, which are illustrated in Figures 5.1 and 5.2. For ACFs, nitrogen adsorption increased with increasing level of activation in the order of ACF10 < ACF15 < ACF20. Both heat-treated and oxidized ACF10 had the same nitrogen adsorption isotherms. Also, heat-treated and oxidized ACF15 exhibited very similar nitrogen adsorption behavior. However, nitrogen adsorption of the heat-treated ACF20 was higher than that of the oxidized one, which was attributed to the fragile structure of ACF20. It appears that some pores of ACF20 collapsed during oxidation and thus decreased the nitrogen adsorption. Nitrogen adsorptions of OLC-H_2 and F400-H_2 showed similar behaviors to the ACF10s (Figure 5.2).

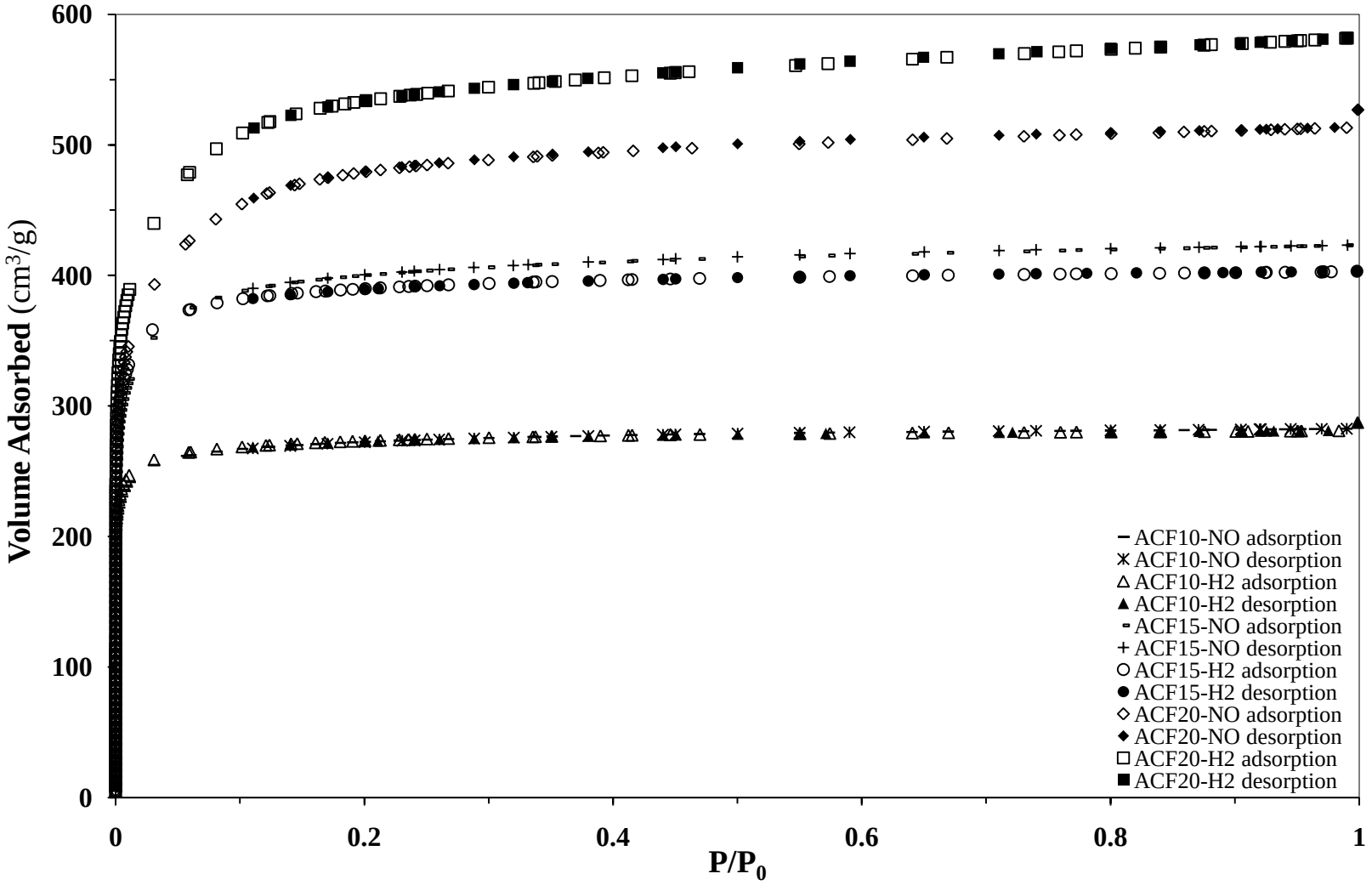

Figure 5.1 Nitrogen adsorption/desorption isotherms of the heat-treated and oxidized ACFs.

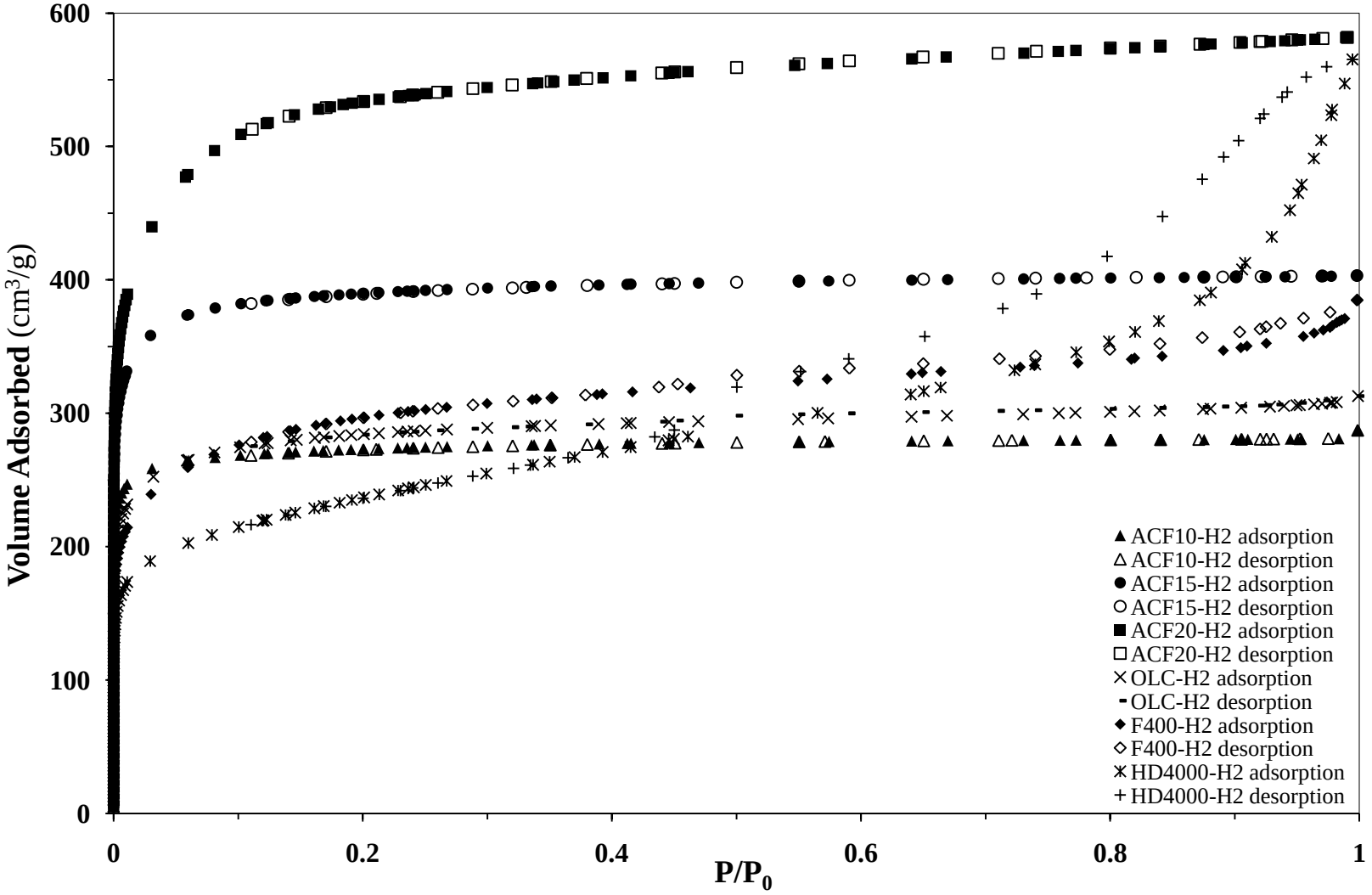

Figure 5.2 Nitrogen adsorption/desorption isotherms of the heat-treated ACFs and GACs.

A sharp increase of adsorption was observed for all nine carbons at relative pressures lower than 0.05, indicating the existence of micropores. It is noteworthy that among all the nitrogen isotherms, only the two coal-based GACs, F400-H_2 and HD4000-H_2, showed desorption hysteresis, which were related to mesopore structure of these carbons [Foster, 1993; Derylo-Marczewska et al., 2004]. The slight hysteresis of F400-H_2 suggested a limited degree of mesoporosity. On the other hand, HD4000-H_2 had a marked hysteresis which demonstrated that capillary condensation was one of the main adsorption mechanisms, and thus, HD4000-H_2 was more mesoporous than the other carbons and had some degree of macropores.

The surface areas and corresponding pore volumes for specific pore size ranges of the adsorbents are summarized in Tables 5.1 and 5.2, respectively. As shown in Table 5.1, all carbons were highly microporous (< 1 nm) with large BET specific surface areas (S_{BET}), with the exception of HD4000-H_2. Among the heat-treated and oxidized ACFs, the surface areas of heat-treated ACFs were slightly higher than those of oxidized ACFs. Heat treatment resulted in higher microporous surface areas (S_{mic}) by 2 to 13% compared to the oxidation of ACF samples. Furthermore, regardless of the surface modification characteristics, the BET surface area increased and PSD broadened in the order of ACF10 < ACF15 < ACF20, which is consistent with the increasing level of activation. Also, S_{mic} of both heat-treated and oxidized ACFs were higher than those of GACs. The same trend was observed for the surface areas of the pores less than 1 nm, which comprised the majority of the pore surface area of the carbons.

Table 5.1 Surface areas and surface area distributions of the adsorbents.*

Adsorbent	**Surface area (m^2 g^{-1})**				**DFT Pore Surface Area (m^2 g^{-1})**					
	S_{BET} [a]	S_{mic} [b]	S_{ext} [c]	S_{BJH} [d]	Total	<1 nm	>1 nm	1-2 nm	2-3 nm	>3 nm
ACF10-H_2	1066	971	95	55	883	789	94	94	0	0
ACF15-H_2	1512	1353	159	90	1253	1072	181	181	0	0
ACF20-H_2	1978	1483	495	249	1612	1056	556	505	40	9
ACF10-NO	1058	946	112	64	879	757	122	118	3	1
ACF15-NO	1526	1281	245	134	1229	926	303	288	12	3
ACF20-NO	1766	1289	477	226	1472	1004	468	420	41	7
OLC-H_2	1080	883	197	117	879	680	199	180	14	5
F400-H_2	1075	662	415	262	899	603	296	231	40	25
HD4000-H_2	838	355	483	514	723	464	259	105	35	79

* Zhang [2010]; [a,b] The specific surface area and microporous surface area obtained from BET; [c] The external surface area obtained from the difference between S_{BET} and S_{mic} ; [d] The specific surface area obtained from BJH model.

Table 5.2 Pore volumes and pore volume distributions of the adsorbents. *

Adsorbent	Pore volume ($cm^3\ g^{-1}$)				DFT Pore Volume Distribution ($cm^3\ g^{-1}$)						Pore diameter (nm)	
	V_t [a]	V_{mic} [b]	V_m [c]	V_{BJH} [d]	Total	<1 nm	>1 nm	1-2 nm	2-3 nm	>3 nm	D_{BJH} [e]	D_{BET} [f]
ACF10-H_2	0.445	0.381	0.064	0.038	0.347	0.278	0.069	0.061	0.000	0.009	1.67	0.56
ACF15-H_2	0.624	0.533	0.091	0.062	0.506	0.379	0.127	0.127	0.000	0.000	1.65	0.61
ACF20-H_2	0.900	0.608	0.292	0.188	0.741	0.303	0.438	0.361	0.046	0.031	1.82	0.74
ACF10-NO	0.437	0.372	0.065	0.045	0.348	0.265	0.083	0.078	0.004	0.001	1.65	0.58
ACF15-NO	0.655	0.511	0.144	0.096	0.533	0.309	0.224	0.200	0.014	0.009	1.72	0.65
ACF20-NO	0.815	0.531	0.284	0.156	0.685	0.299	0.386	0.304	0.050	0.032	1.85	0.74
OLC-H_2	0.484	0.353	0.131	0.094	0.404	0.235	0.169	0.126	0.015	0.028	3.22	1.79
F400-H_2	0.596	0.277	0.319	0.243	0.511	0.180	0.331	0.165	0.049	0.114	3.72	2.22
HD4000-H_2	0.875	0.155	0.720	0.737	0.663	0.144	0.519	0.073	0.045	0.401	5.74	4.18

* Zhang [2010]; [a,b] The total pore volume and micropore volume obtained from *t*-plot model; [c] The total of meso- and macropore volumes ; [d] The total pore volume obtained from BJH model; [e,f] Average pore diameters obtained from BJH and BET methods, respectively.

Table 5.2 shows the pore volumes and pore volume distributions of the carbons. Considering their dimensions (Table 4.2), pore volumes less than 2 nm might be the adsorption sites for the selected SOC molecules and comprised a large portion of the carbons, except that of HD4000-H_2. While F400-H_2 had some amount of pores larger than 3 nm, the volumes of pores larger than 3 nm were negligible for all ACFs and OLC-H_2. On the other hand, HD4000-H_2 had a high amount of pores larger than 3 nm, and thus, was the least microporous carbon compared to the other carbons. Barrett-Joyner-Halenda (BJH) and BET methods were employed to obtain average pore diameters of the carbons. The BJH method was used for pores with diameter in the range of 2 - 300 nm (D_{BJH}). Both BET and BJH methods exhibited an identical order, which was larger for the GACs and smaller for the ACFs, and pore diameter increased with increasing level of activation. Furthermore, the results showed that modification of the ACFs by either heat-treatment or oxidation did not change the pore diameters. Overall, pore diameters of the carbons decreased in the order of HD4000-H_2 > F400-H_2 > OLC-H_2 > ACF20-H_2 = ACF20-NO > ACF15-H_2 ≈ ACF15-NO > ACF10-H_2 ≈ ACF10-NO.

5.1.2 Surface Chemistry of Carbons

The surface chemistry characterization results of the adsorbents are provided in Table 5.3. In comparison to the oxidized carbons, the heat-treated carbons had significantly higher pH_{PZC} values. However, when comparing within each group of carbons, i.e., the heat-treated ACFs versus heat-treated GACs, pH_{PZC} values were relatively similar. The sum of the carbon, hydrogen, nitrogen, and oxygen contents represented approximately 87-98 % of the total carbon mass for all the carbons, which

indicated that the ash contents of the carbons were small. Lower ash content is preferable, since ash constituents can create hydrophilic sites on the carbon surface [Arafat et al., 1999].

Table 5.3 Chemical characteristics of the adsorbent surfaces.

Adsorbent	**pH_{PZC}**	**Elemental Analysis (%)**			
		C	H	N	O
ACF10-H_2	9.94	95.46	0.87	0.00	0.15
ACF15-H_2	10.08	96.11	0.64	0.00	0.10
ACF20-H_2	10.13	96.67	0.64	0.07	0.08
ACF10-NO	3.15	75.79	1.79	0.68	16.62
ACF15-NO	3.08	70.11	1.60	0.77	15.82
ACF20-NO	3.15	75.09	0.72	0.88	10.61
OLC-H_2	10.26	96.10	0.62	0.26	0.08
F400-H_2	10.23	90.56	0.49	0.57	0.05
HD4000-H_2	9.93	90.02	0.78	0.74	0.27

Oxygen and nitrogen contents of the studied carbons indicated that while the heat-treated GACs and ACFs had similar oxygen contents, the heat-treated GACs had relatively higher nitrogen contents than those of ACFs. Compared to the oxidized carbons, the heat-treated carbons had significantly lower oxygen contents. As a consequence, low oxygen and nitrogen contents exhibited basic hydrophobic surfaces with high pH_{PZC} values, whereas high oxygen and nitrogen contents resulted in carbons with acidic hydrophilic character and low pH_{PZC}.

Water vapor adsorption experiments were conducted to obtain information about the surface hydrophobicity of the carbons, and the results are shown in Figures 5.3 and 5.4. The water vapor uptakes at the low relative pressure range (P/P_0 is below 0.4) suggest the presence of the surface functional groups, and thus, are related to the water cluster formation on the hydrophilic sites. Heat treatment causes the degradation of surface functionalities, and makes the carbons less hydrophilic [Kaneko et al., 1999; Karanfil and Dastgheib, 2004]. As displayed in Figure 5.3, at the low relative pressure range, the oxidized ACFs demonstrated higher affinities to water than the heat-treated ones. This confirms that the oxidized carbons were more hydrophilic, while the heat-treated carbons were more hydrophobic. The comparison of the heat-treated ACFs and GACs is given in Figure 5.4. Both water vapor adsorption experiments and elemental analysis demonstrated that affinity of each heat-treated carbon to water was similar, indicating the six carbons had similar amounts of oxygen contents and low surface polarities.

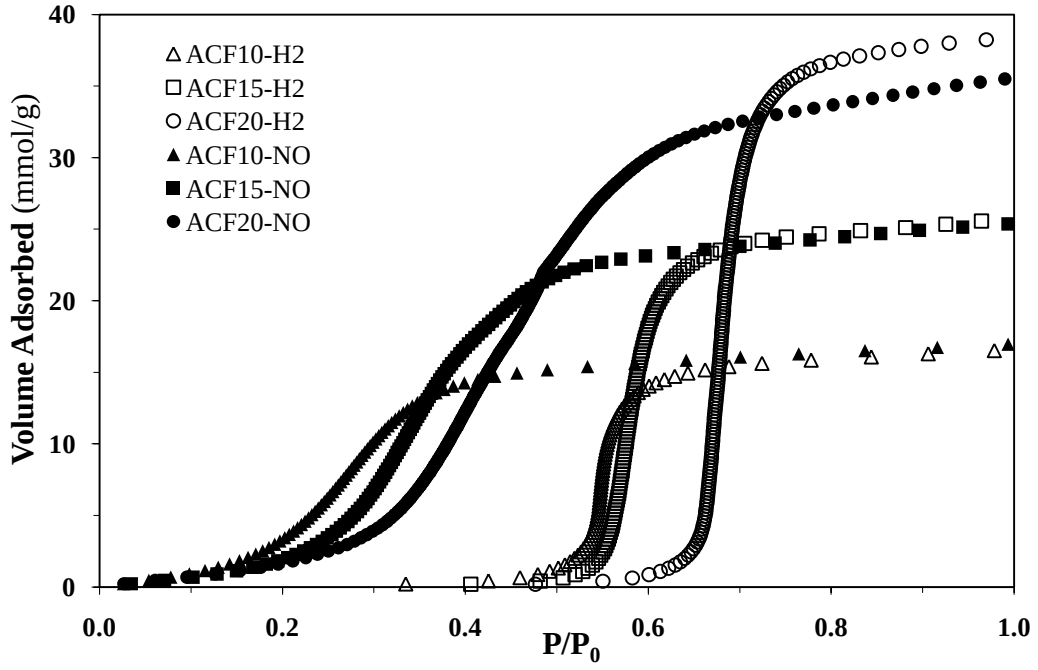

Figure 5.3 Water vapor adsorption isotherms of the heat-treated and oxidized ACFs.

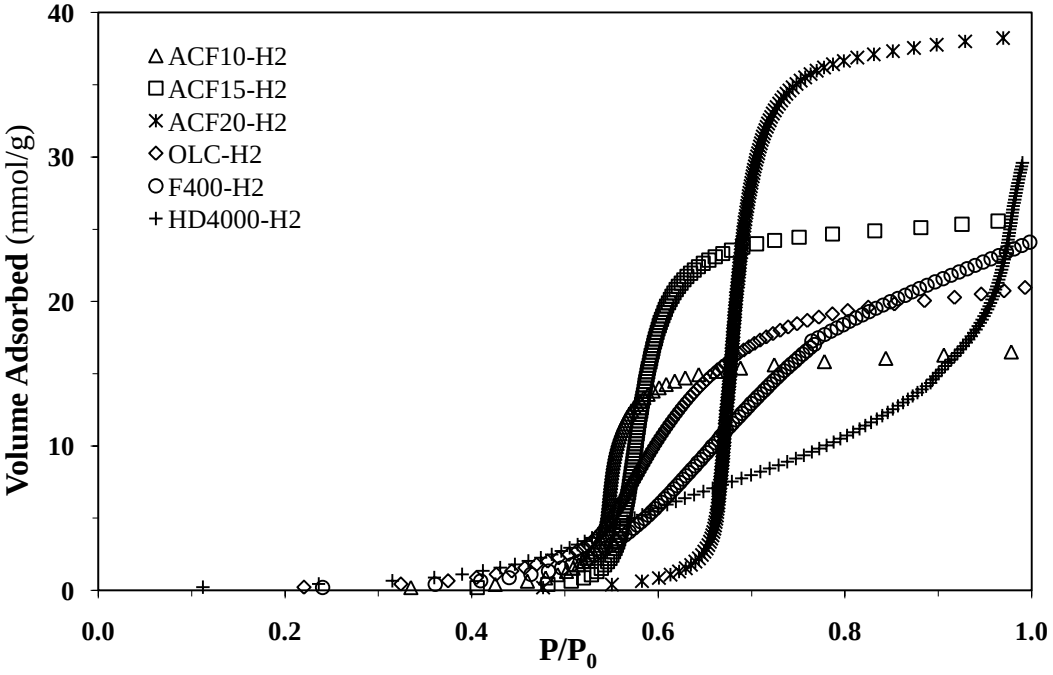

Figure 5.4 Water vapor adsorption isotherms of the heat-treated ACFs and GACs.

5.2 Modeling of the Isotherm Data

In order to investigate the objectives of this study, single-solute isotherm experiments were conducted for the selected synthetic organic compounds (SOCs) with heat-treated and oxidized ACFs, and heat-treated GACs. To quantitatively describe the isotherm results, four nonlinear isotherm models, Freundlich (FM), Langmuir (LM), Langmuir-Freundlich (LFM), and Polanyi-Manes model (PMM), and a linear isotherm model were applied to the experimental data by using Microsoft Office Excel 2007 [Carter, 1993; Zhang et al., 2010]. Residual root mean square error (RMSE) and coefficient of determination (r^2) were used to evaluate the goodness of the fits.

$$RMSE = \sqrt{\frac{1}{m}\sum_{i=1}^{N}(q_{e,exp} - q_{e,fit})^2} \tag{5.1}$$

Where, N is the number of experimental data points, m is the degree of freedom ($m = N - 2$ for the two-parameter LM and FM; $m = N - 3$ for the three-parameter LFM and PMM), $q_{e,exp}$ is the experimental equilibrium concentration and $q_{e,fit}$ is the fitted equilibrium concentration.

The results of the nonlinear modeling for benzene (BNZ), biphenyl (BP), phenanthrene (PHE) and 2-hydroxybiphenyl (2HB) are summarized in the Appendix A. It was observed that for most of the isotherms, the three-parameter LFM and PMM had lower RMSE and higher r^2 values than the LM and FM. However, the FM with two-parameters had the lowest RMSE values for BNZ on three GACs and ACF20-H_2, and had the highest r^2 value on OLC-H_2. For BP, the LM with two-parameters showed the

lowest RMSE values on ACF10-H_2 and ACF15-NO, and the highest r^2 values on the ACF10-NO and HD4000-H_2. While the LM had the lowest RMSE values for PHE on three heat-treated ACFs, the FM had the lowest RMSE for PHE on the HD4000-H_2. Finally, the FM had the highest r^2 for 2HB on ACF10-H_2. These exceptions demonstrated the overparametrization in some cases by the three-parameter LFM and PMM fitting. As a combination of the FM and the LM, the LFM converts to the LM at $n = 1$ and to the FM at low solute concentrations ($K_S C_e^n << 1$). The model estimation with the LM deviated from experimental data at a low concentration range. This suggested that the LM was not applicable to the collected experimental data, which also explained the failure of the LFM in some of the cases. PMM assumes that adsorption is controlled by nonspecific dispersive interactions, which means this model may be unable to predict adsorption that involves specific interactions, such as the formation of hydrogen-bond and electron donor-acceptor complexes between adsorbates and oxygen-containing functional groups of adsorbents.

Overall, based on the results obtained from the data simulations, the linear form of the FM was selected to model the experimental data among the five isotherm models and its model parameters had meaningful results; therefore, it was used to analyze the data in this study. The linear form of Freundlich model used for simulating data is

$$lnq_e = lnK_F + n\, lnC_e \tag{5.6}$$

Since K_F is a unit-capacity parameter, it is sensitive to the concentration units which are employed to calculate it (e.g., mg/L or mmol/L). As a result, K_F values may have no meaningful relationships to the studied range of the experimental data [Walters

and Luthy, 1984]. In order to overcome this problem, Carmo et al. (2000) proposed a modified Freundlich model (Equation 5.7) and suggested a unit-equivalent Freundlich coefficient by normalizing C_e to the water solubility (C_s) of the adsorbate.

$$q_e = K_{FS}(C_e/C_s)^n \quad (5.7)$$

Where, K_{FS} is a parameter independent of the concentration units and represents the effective overall adsorption capacity of the adsorbent at saturated concentration. For adsorbates with high solubilities, an adjustment was made for calculating the K_{FS}. To avoid the unreasonably higher values, 1% of the solubilities ($C_{s(1\%)}$) were taken into account as reference points instead of using water solubility normalization data directly [Carrott et al., 2005]. The 95% confidence intervals and standard errors for the isotherms are provided in the Appendix B.

5.3 The Role of Adsorbent Physical Characteristics on SOC Adsorption

Adsorption of BNZ, BP and PHE on the heat-treated ACFs and GACs was compared to examine the effects of carbon physical characteristics (i.e., surface area, surface area distribution, pore size, pore distribution) on SOC adsorption by excluding the chemical interactions. The surface chemistries of the carbons were relatively similar. All six carbons had basic surfaces with $pH_{PZC} \approx 10$ and low amounts of oxygen (Table 5.3) and low surface polarities (Figure 5.4). Mass-basis, solubility-normalized and surface area-normalized adsorption capacities of the adsorbates, along with r^2 values, were examined to explain the adsorption phenomena, and capacities were represented by K_F, K_{FS}, and Q, respectively (Table 5.4). While K_F values provide information for the

isotherm trends at low concentrations, K_{FS} values (i.e., solubility-normalized isotherms) provide information about the overall available adsorption sites on the carbon surface at or near saturation capacities. The Q was obtained by dividing the K_{FS} values by the S_{BET} values of the carbons.

Table 5.4 Freundlich isotherm parameters of BNZ, BP and PHE.

SOC	**Adsorbent**	K_F [a] [(mg/g)/Ce^n] (μg/L)	K_F [a] [(mg/g)/Ce^n] (mg/L)	K_{FS} [b] (mg/g)	Q [c] (mg/m^2)	V_O [d] (mL/g)	V_O/V_t [e]	n	r^2
BNZ	ACF10-H_2	1.80	65	290	0.272	0.330	0.742	0.52	0.976
	ACF15-H_2	2.91	80	318	0.210	0.362	0.580	0.48	0.972
	ACF20-H_2	3.11	93	382	0.193	0.435	0.483	0.49	0.971
	OLC-H_2	1.39	54	245	0.227	0.279	0.576	0.53	0.979
	F400-H_2	0.95	43	212	0.197	0.241	0.404	0.55	0.972
	HD4000-H_2	0.32	25	156	0.186	0.177	0.203	0.63	0.984
BP	ACF10-H_2	13.99	262	565	0.530	0.569	1.280	0.42	0.954
	ACF15-H_2	17.02	421	976	0.646	0.983	1.576	0.46	0.949
	ACF20-H_2	19.45	711	1825	0.923	1.840	2.045	0.52	0.946
	OLC-H_2	9.98	344	870	0.806	0.877	1.812	0.51	0.905
	F400-H_2	12.87	290	656	0.610	0.662	1.110	0.45	0.894
	HD4000-H_2	13.04	263	578	0.690	0.583	0.666	0.44	0.897
PHE	ACF10-H_2	2.84	197	209	0.196	0.196	0.441	0.61	0.960
	ACF15-H_2	7.41	404	427	0.282	0.402	0.644	0.58	0.957
	ACF20-H_2	13.65	574	604	0.305	0.568	0.631	0.54	0.886
	OLC-H_2	0.67	384	419	0.388	0.367	0.759	0.92	0.989
	F400-H_2	2.12	239	255	0.237	0.240	0.403	0.68	0.982
	HD4000-H_2	1.86	303	325	0.388	0.306	0.349	0.74	0.898

[a] Mass-basis adsorption affinity expressed in different units; [b] Solubility normalized adsorption capacity (K_F values at saturated concentrations of SOCs). Due to its high solubility, BNZ was simulated with 1% of its water solubility; [c] Surface area normalized adsorption capacity; [d] The volumes occupied by adsorbed SOCs; [e] The pore volume occupancy.

For BNZ, the K_F values indicated that ACFs had higher adsorption affinities than GACs, which was consistent with the higher specific surface areas and microporosity of ACFs. While more than 75% of the pores in ACFs are microporous (i.e., S_{mic}/S_{BET} in Table 5.1), the corresponding values are 40, 60, and 80% for HD4000-H_2, F400-H_2, and OLC-H_2, respectively.

Since the dimensions of the BNZ molecule is smaller than 1 nm (7.4 Å × 6.7 Å × 3.4 Å), both PSDs of the adsorbents and the pore volume in pores less than 1 nm are important for the adsorption of BNZ. Therefore, pore filling in pores less than 1 nm is expected to be the main mechanism for the adsorption of BNZ. As indicated by the K_F values in Table 5.4 and adsorption isotherms in Figure 5.5, BNZ uptake was in the order of ACF20-H_2 ≥ ACF15-H_2 > ACF10-H_2 > OLC-H_2 > F400-H_2 > HD4000-H_2. This order was consistent with the order of S_{mic}, S (<1nm) and micropore volume (V_{mic}) of the carbons (Tables 5.1 and 5.2). Therefore, at low concentration range, BNZ adsorption increased with the increase in micropore volume or pore volume in pores < 1nm. The same conclusions were also obtained for K_{FS} values. Because the aqueous solubility of BNZ is very high (Table 4.2), 1% of BNZ solubility was calculated and used in the solubility normalization for each carbon. The results indicated that there was no restriction for BNZ molecules to access into the pores; and thus, adsorption increased with increasing specific surface areas, especially with S_{mic}.

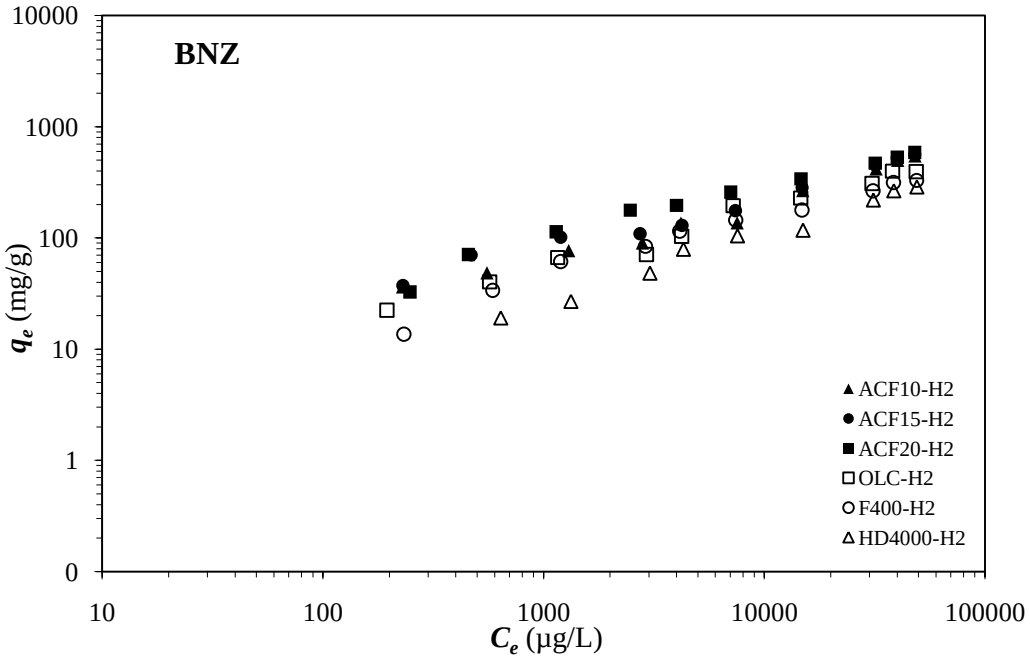

Figure 5.5 BNZ adsorption isotherms for heat-treated ACFs and GACs.

The volumes occupied by adsorbed SOCs (V_O) were calculated by dividing the K_{FS} values with the densities of SOCs. In order to examine the pore volume occupancy, ratios of V_O to total pore volume (V_t) were calculated for each carbon. As indicated by the V_O/V_t values in Table 5.4, the order of pore volume occupancy of BNZ was consistent with the order of micropore fractions (i.e., S_{mic}/S_{BET} in Table 5.1) of the carbons, which was ACF10-H_2 (91%) > ACF15-H_2 (89%) > OLC-H_2 (82%) > ACF20-H_2 (75%) > F400-H_2 (62%) > HD4000-H_2 (42%). The carbons with higher micropore volumes had higher pore volume occupancies.

To further analyze the BNZ adsorption, different relationships between structural parameters of the adsorbents and their adsorption capacities were examined. The K_{FS} of each carbon was plotted to different structural parameters which were listed in Tables 5.1

and 5.2. These structural parameters were S_{BET}, S_{mic}, S (<1nm), S (>1nm), S (1-2 nm), V_{total}, V_{mic}, V (<1nm), V (>1nm), and V (1-2 nm). The observed strong correlations between K_{FS} and these parameters are shown in Figures 5.6 to 5.10. The poor relationships are not shown in here; however, they are summarized in the Appendix C.

BNZ adsorption was strongly correlated with S_{BET}, S_{mic} V_{mic} of the carbons, and especially surface areas and pore volumes that are in pores smaller than 1 nm. This is not surprising given that BNZ is a small molecule, and it can easily fill the micropores of adsorbents. These strong correlations independent of pore structures (slit-shaped GAC pores vs. elliptical ACF pores) also indicated that the type of pore structure did not play a major role in BNZ adsorption and pore filling was the main mechanism of adsorption.

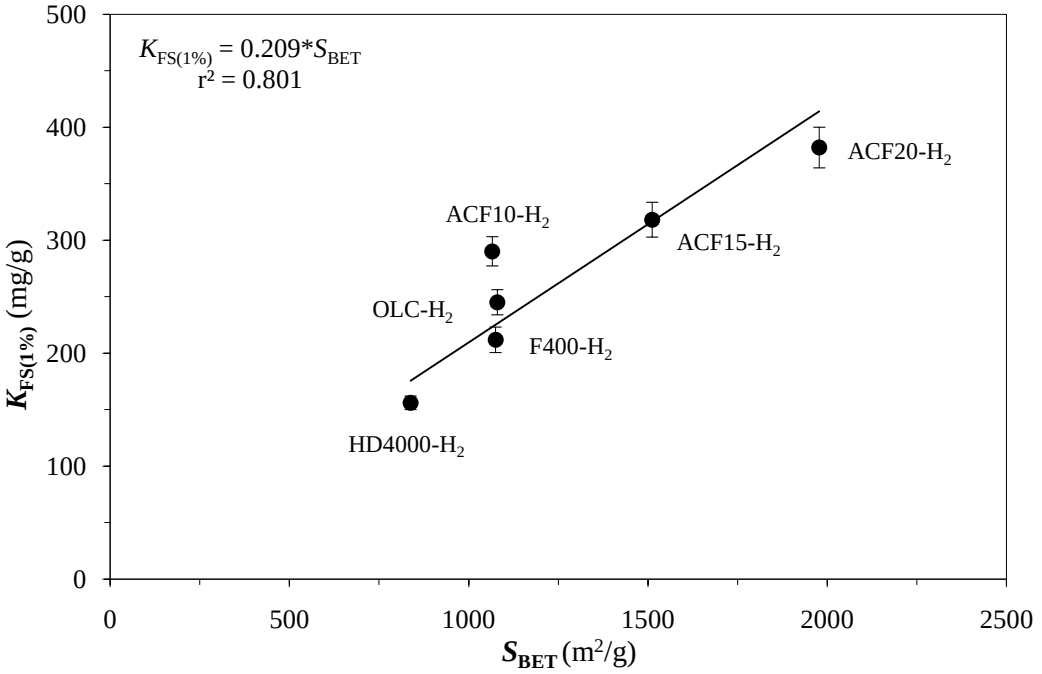

Figure 5.6 Correlation between the BET surface areas of the carbons and their BNZ adsorption capacities. (Error bars indicate the 95% confidence intervals.)

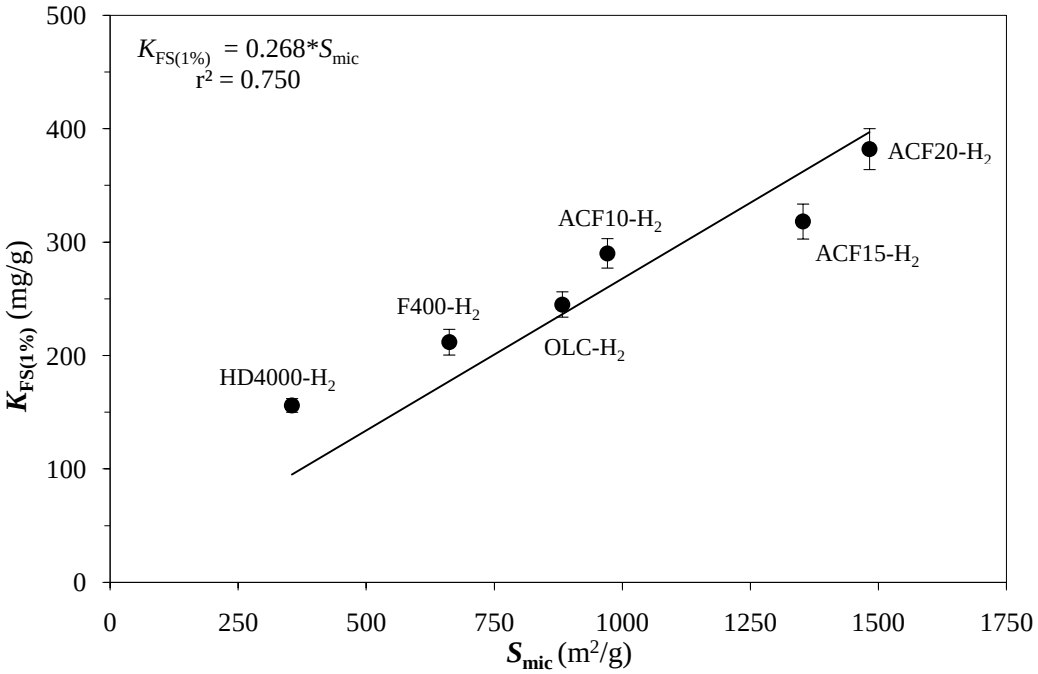

Figure 5.7 Correlation between the microporous surface areas of the carbons and their BNZ adsorption capacities. (Error bars indicate the 95% confidence intervals.)

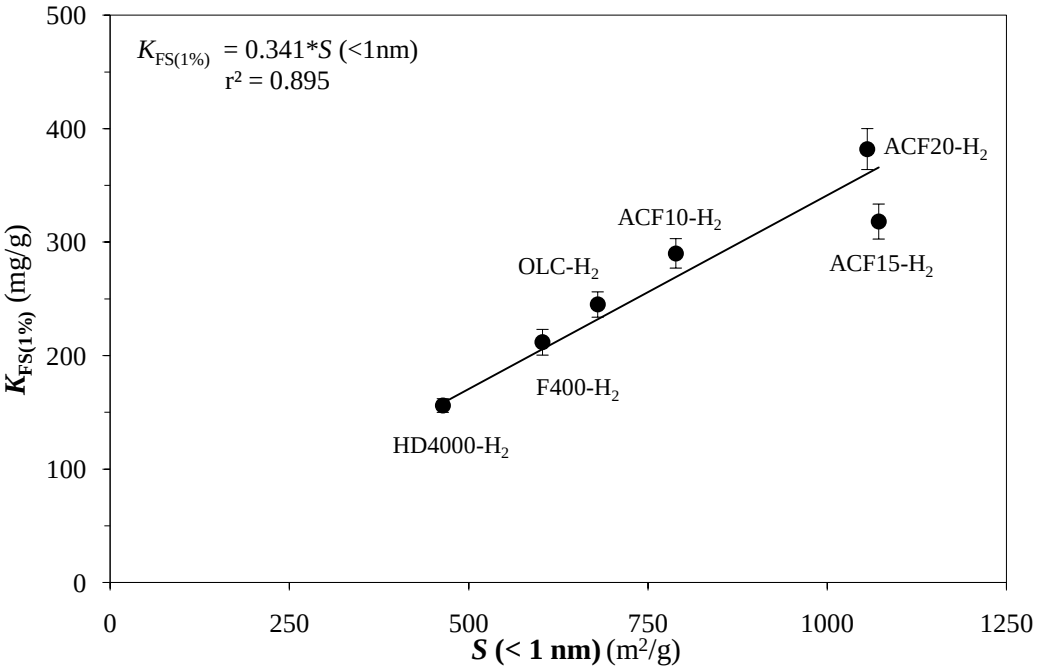

Figure 5.8 Correlation between the surface areas in pores less than 1 nm of the carbons and their BNZ adsorption capacities. (Error bars indicate the 95% confidence intervals.)

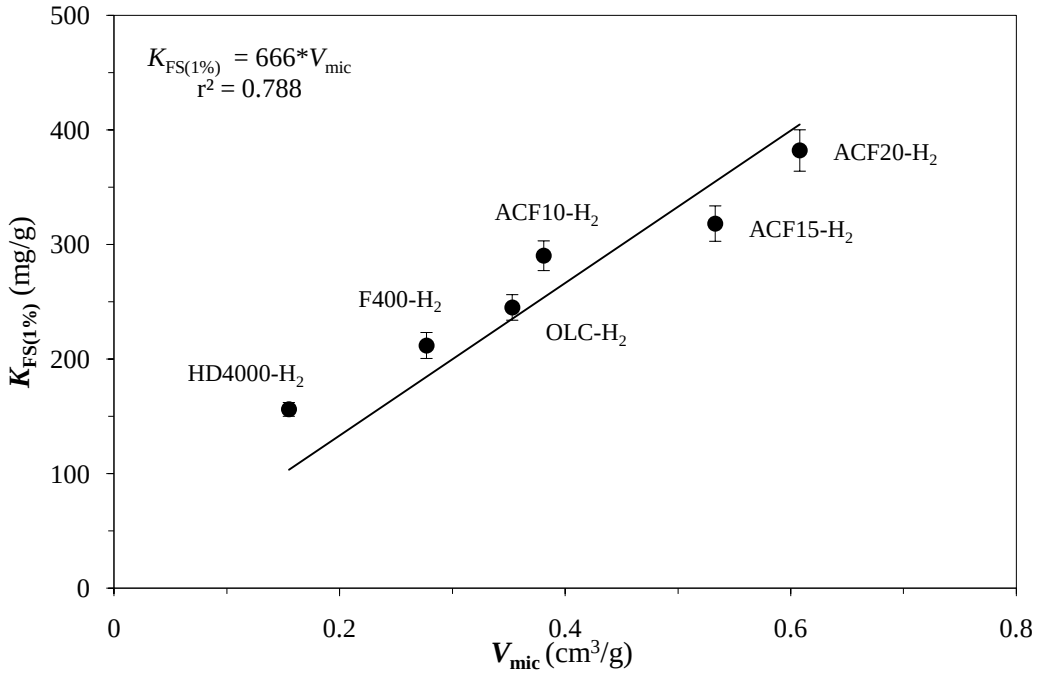

Figure 5.9 Correlation between the micropore volumes of the carbons and their BNZ adsorption capacities. (Error bars indicate the 95% confidence intervals.)

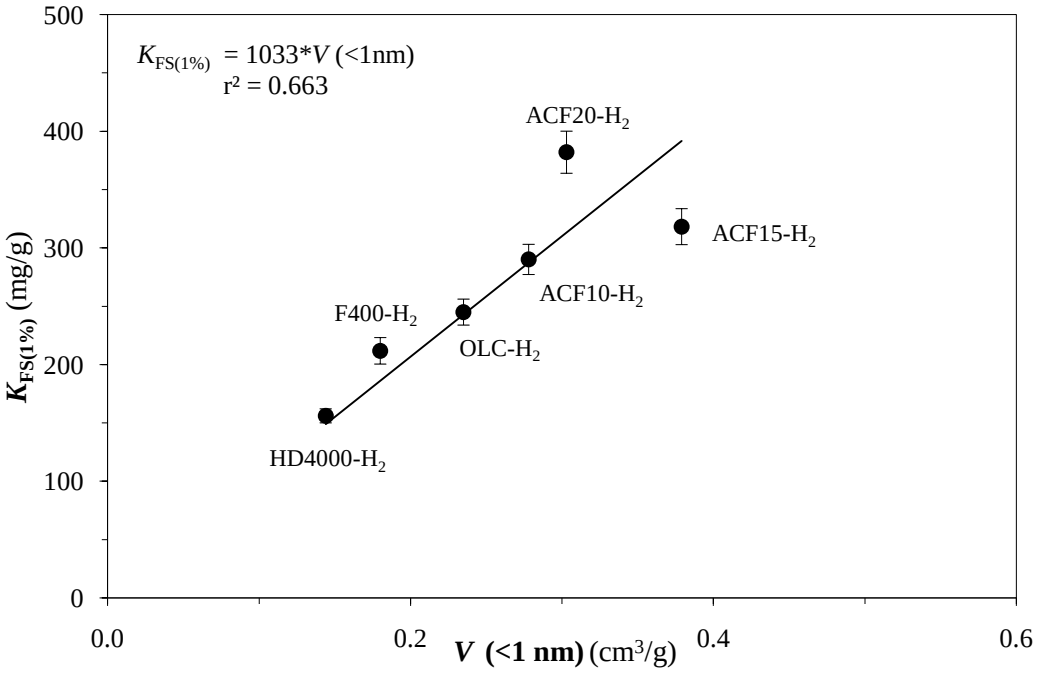

Figure 5.10 Correlation between the pore volumes in pores less than 1 nm of the carbons and their BNZ adsorption capacities. (Error bars indicate the 95% confidence intervals.)

For BP, the mass-basis adsorption Freundlich affinities (K_F values) followed the order of ACF20-H_2 > ACF15-H_2 > ACF10-H_2 > HD4000-H_2 ≈ F400-H_2 > OLC-H_2 (Table 5.4). This order did not follow the order of the surface areas or the pore volumes of the carbons. The three ACFs showed similar uptakes at the low concentration range, while the capacity at high concentrations was in the order of ACF20-H_2 > ACF15-H_2 > ACF10-H_2 (Figure 5.11).

The solubility-normalized adsorption capacities (K_{FS}) were in the order of ACF20-H_2 > ACF15-H_2 > OLC-H_2 > F400-H_2 > HD4000-H_2 ≈ ACF10-H_2. HD4000-H_2 had the lowest surface area among all the carbons, while ACF10-H_2 had 75% of its pore volume in pores (11.8 Å × 6.8 Å × 4.7 Å) smaller than 1 nm. Therefore, their low K_{FS} values were attributed to the molecular sieve effect on ACF10-H_2 and low surface area of HD4000. For example, on a mass-basis isotherm, although ACF10-H_2 has higher adsorption capacities than GACs at low concentrations, it exhibited the lowest BP uptakes at the highest concentrations, indicating that ACF10-H_2 reached saturation and did not have more pore space to accommodate additional BP molecules. Coconut-based carbons exhibit better adsorptive capacities for small compounds than the coal-based carbons [Mangun et al., 1999]. In fact, the solubility normalized and surface area normalized adsorption capacities of coconut-based OLC-H_2 were higher than those of coal-based F400-H_2 and HD4000-H_2 (Table 5.4).

Correlations between BP adsorption and structural parameters of the carbons were also investigated. The best correlation was observed between K_{FS} and S_{BET}, if ACF10-H_2

was left out of the correlation due to the molecular sieve effect observed for this adsorbent (Figure 5.12).

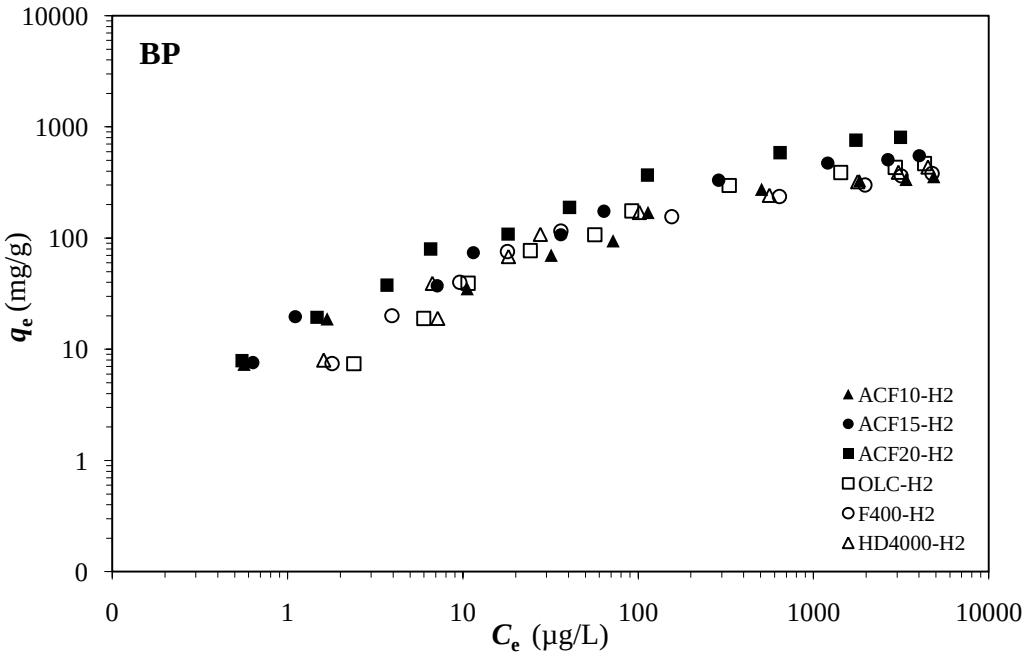

Figure 5.11 BP adsorption isotherms for heat-treated ACFs and GACs.

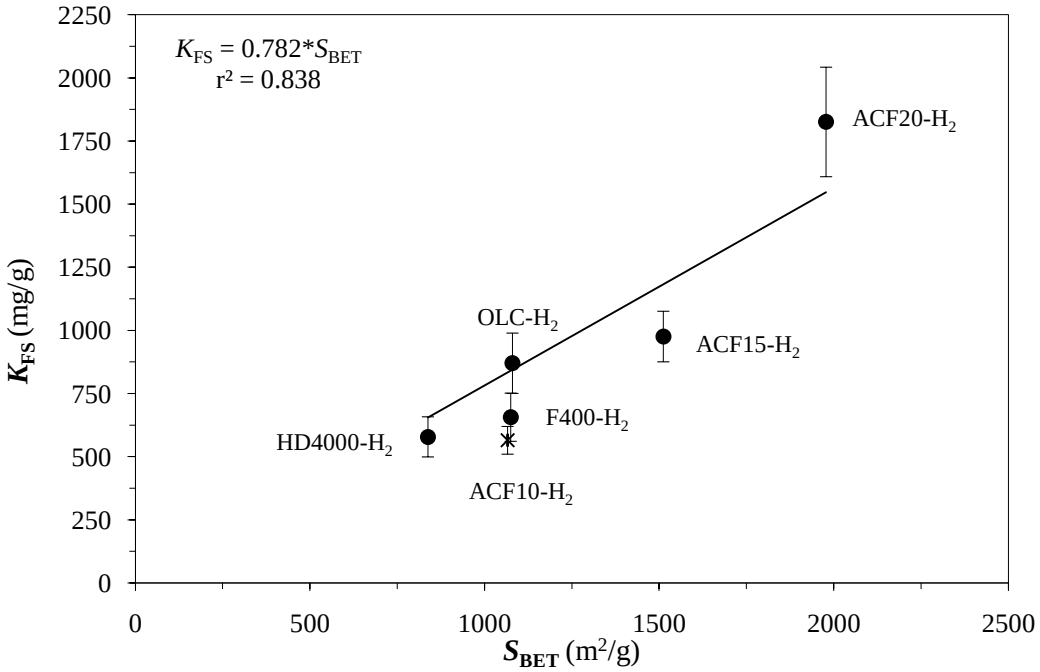

Figure 5.12 Correlation between the BET surface areas of the carbons and their BP adsorption capacities (ACF10-H_2 is shown but not included in the correlation). (Error bars indicate the 95% confidence intervals.)

The adsorption isotherms for PHE are illustrated in Figure 5.13 and isotherm parameters are summarized in Table 5.4. The Freundlich parameter K_F was in the order of ACF20-H_2 > ACF15-H_2 > ACF10-H_2 ≈ F400-H_2 ≈ HD4000-H_2 > OLC-H_2. It appears that neither pore volumes nor surface areas can be used as a predictor of PHE uptake. However, as it was observed for BNZ and BP adsorption, highly microporous ACFs had higher adsorption affinities than those of the GACs. Based on the solubility and surface area normalized adsorption data, adsorption capacities (K_{FS} and Q) of PHE on ACF10-H_2 was the lowest, even though S_{mic} of ACF10-H_2 was higher than that of GACs.

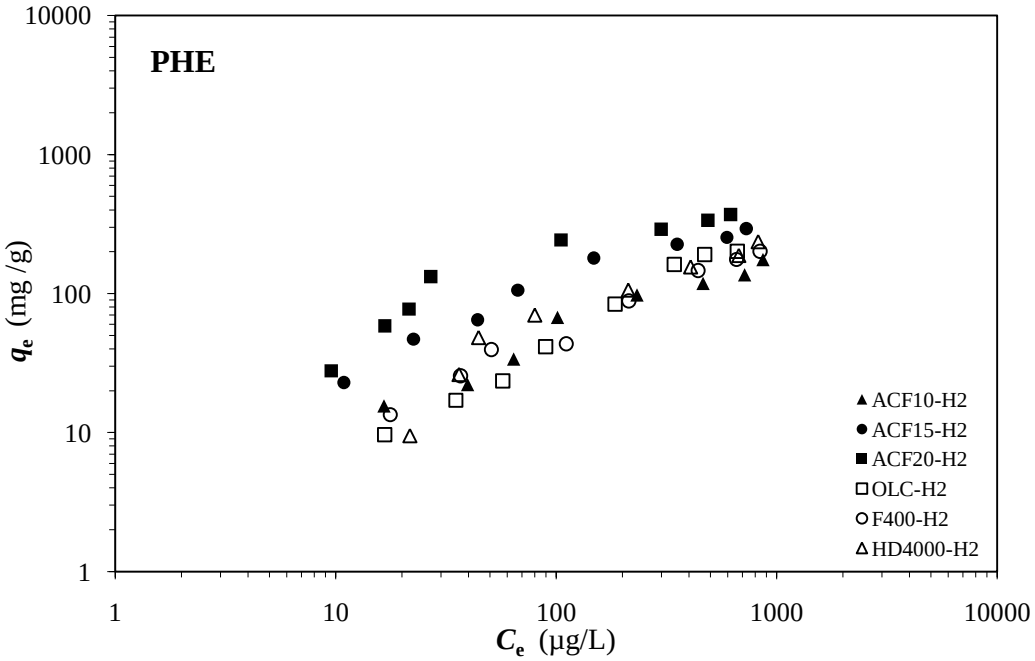

Figure 5.13 PHE adsorption isotherms for heat-treated ACFs and GACs.

Results indicated that molecular sieving occurred on the adsorption of ACF10-H_2, similar to BP. Since the molecular dimensions of PHE are 11.7 Å × 8.0 Å × 3.4 Å, pore volumes between 1-2 nm were the likely adsorption sites of PHE. As it was mentioned earlier, more than 75% of the pores in ACF10-H_2 are less than 1 nm. Therefore, there are not enough available contact surfaces for all the PHE molecules to adsorb on ACF10-H_2. The molecular sieve effect occurs when the pore width is narrower than the molecular size of the adsorbate or the shapes of the pores do not allow the molecules to enter into the micropores [Bandosz, 2006]. While it is the smallest dimension of the adsorbate that determines its accessibility to the slit-shaped pores (i.e., GACs), the second-widest dimension of the adsorbate is the determining factor for cylindrical or ellipsoidal pores (i.e., ACFs). Since the second-widest dimension of PHE is 0.80 nm, molecular sieve effect is very likely to play a key role in PHE adsorption by ACF10-H_2.

As for BP, the best correlation between K_{FS} and structural parameters for PHE was observed between K_{FS} and S_{BET} (Figure 5.14).

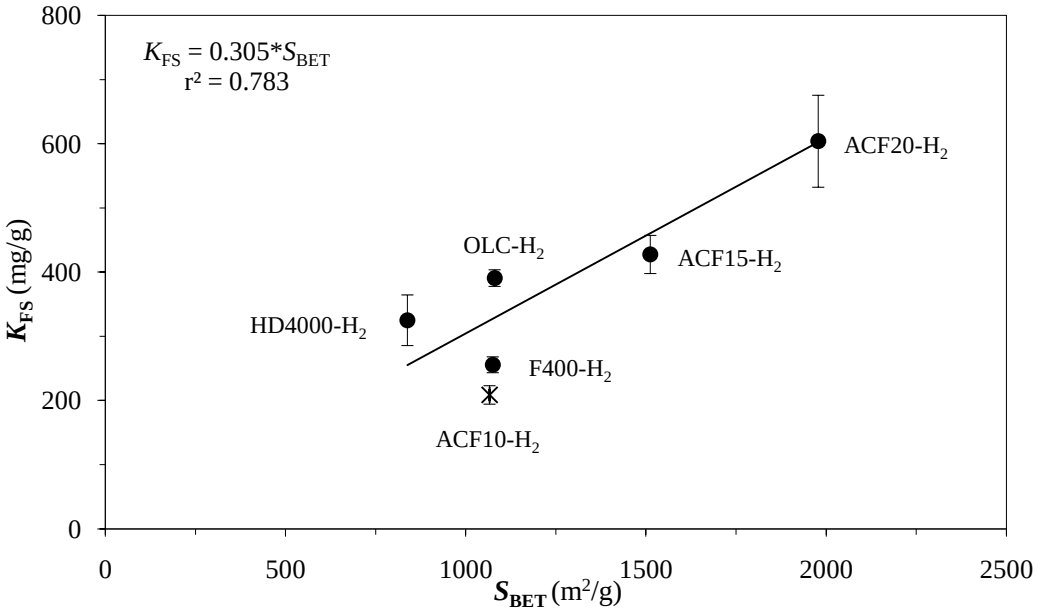

Figure 5.14 Correlation between the BET surface areas of the carbons and their PHE adsorption capacities (ACF10-H_2 is shown but not included in the correlation). (Error bars indicate the 95% confidence intervals.)

Overall, the mass-basis Freundlich equilibrium constants for each of the adsorbates were higher for ACFs than for GACs. ACFs exhibited higher adsorption affinities for adsorbates with low-molecular sizes than did GACs, because of the higher specific surface areas and microporous structures of ACFs [Kaneko et al., 1989; Le Cloirec et al., 1997; Moreno-Castilla, 2004]. Micropores played an important role in the adsorptions due to the overlapping of adsorption potentials between the opposite walls. Therefore, there were much stronger adsorption energies in micropores than those in mesopores and macropores which usually act as diffusion channels [Dubinin, 1989]. Results also indicated that the accessible pore size region for BNZ was in pores less than 1 nm and pore filling played an important role on the adsorption of BNZ. On the other

hand, accessible pore size regions for BP and PHE were determined to be approximately 1 - 2 nm, and molecular sieving occurred on the adsorption of BP and PHE as a result of their molecular dimensions.

5.4 The Role of SOC Characteristics on Adsorption by ACs

The adsorption of BNZ, BP, PHE on the heat-treated ACFs and GACs, and the adsorption of BP and 2HB on the heat-treated and oxidized ACFs were compared to investigate the effects of the adsorbate characteristics on the adsorption. For the comparison, adsorption of different SOCs on one type of carbon was examined. The adsorption of SOCs was evaluated on the logarithmic scale by plotting the q_e values as ordinate and the solubility normalized concentrations, C_e / C_s, as abscissa, to eliminate the differences induced from the different solubilities of the compounds.

As mentioned earlier, the presence of the functional groups, molecular conformation, weight, size, polarity, and solubility of an adsorbate affect the adsorption. On the other hand, for an adsorbent, while pore and surface structures of the adsorbent determine the space availability to the adsorbates, its surface chemistry influences the chemical affinity to the adsorbates. Since the six heat-treated carbons had relatively comparable pH_{PZC} values as well as oxygen and nitrogen contents, their surface areas and pore size distributions are expected to play an important role in the adsorption rather than their surface chemistries. Figures 5.15 and 5.16 display the adsorption of BNZ, BP, and PHE on the heat-treated ACFs and GACs. The uptakes of the SOCs followed the order of BNZ > BP > PHE for all heat-treated carbons. Such order of uptake clearly demonstrates the effects of molecular dimension and molecular conformation of these three SOCs.

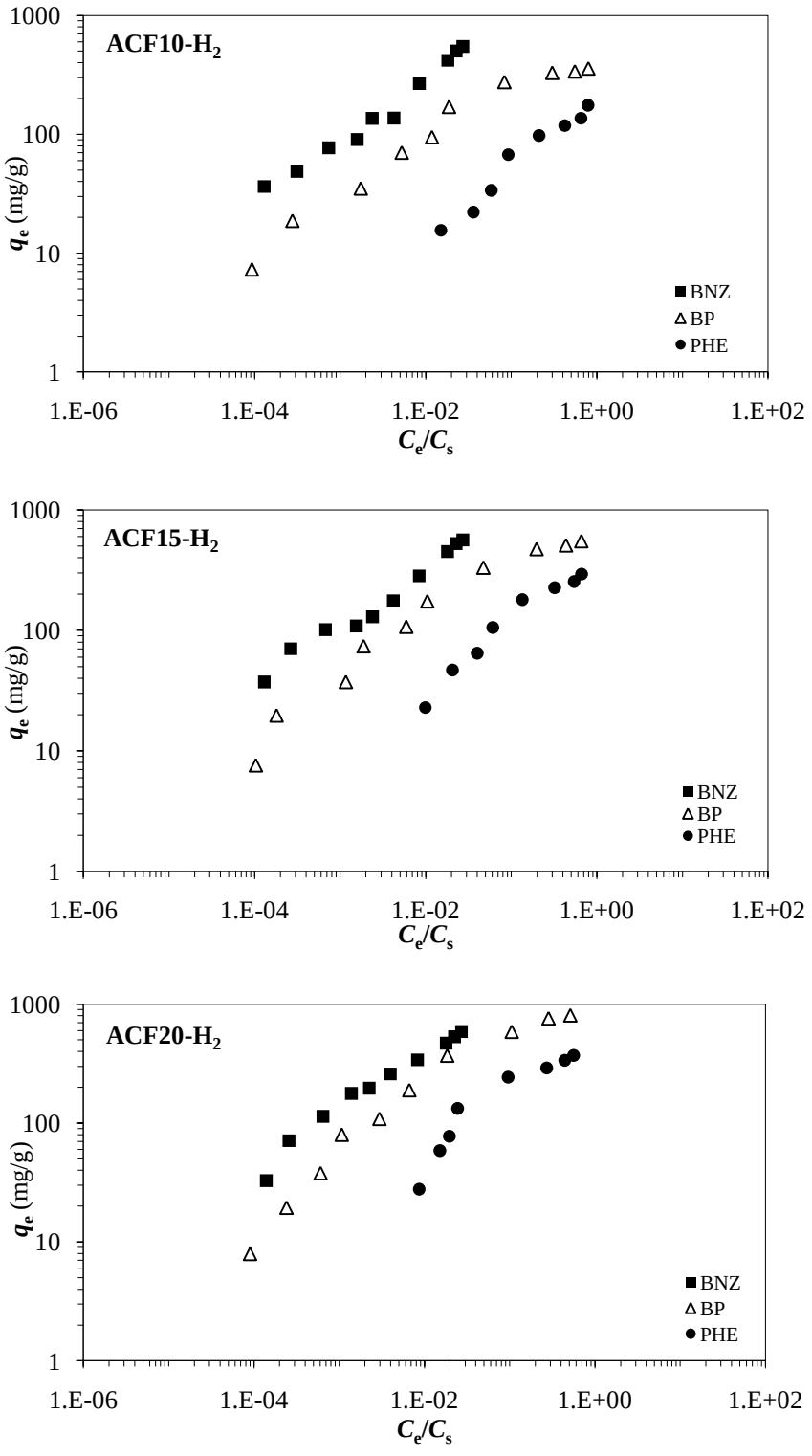

Figure 5.15 Comparison of the BNZ, BP and PHE solubility-normalized adsorption isotherms on the ACFs.

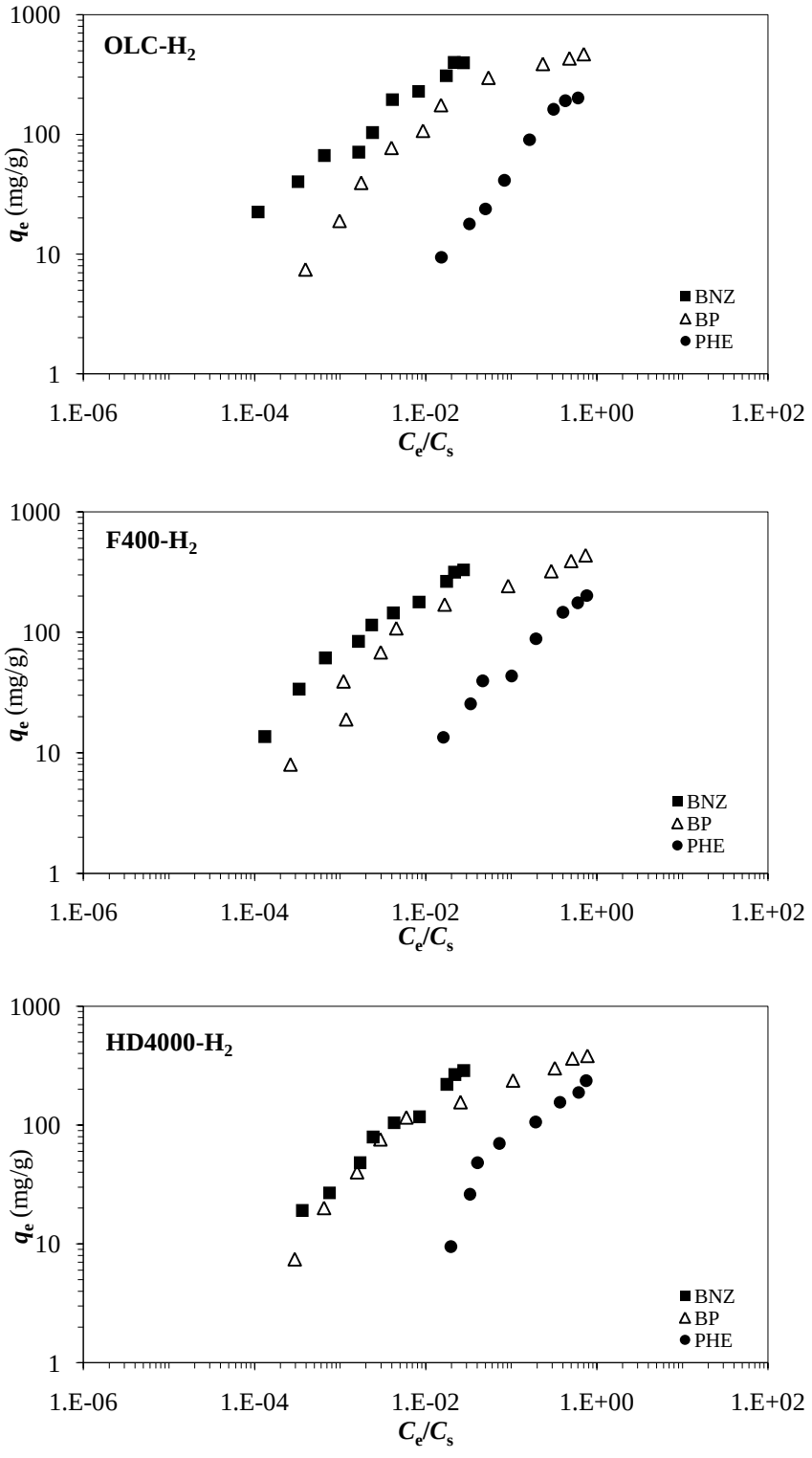

Figure 5.16 Comparison of the BNZ, BP and PHE solubility-normalized adsorption isotherms on the GACs.

Not surprisingly, the uptakes increased with decreasing molecular dimension of each compound. The molecular dimension with respect to the PSD of an adsorbent determines the accessible surface area or pore volume for the adsorption of an adsorbate. BNZ (the smallest SOC in this study) adsorption was always higher than those of BP and PHE. Even though PHE and BP had similar physicochemical properties, the adsorption potentials of these compounds were significantly different. Adsorption affinities of BP were approximately two times higher than PHE for all six carbons (Table 5.4). Between these two compounds, BP has the smaller width, which is also considered as the second-widest dimension of a compound. This feature provides BP a higher accessibility to the ACFs and pores can be filled better by BP than that of PHE, since it is the second-widest dimension of the adsorbate that determines its accessibility to the ellipsoidal pores. On the other hand, the smallest dimension, also known as the thickness, of an adsorbate determines its accessibility to the slit-shaped pores, such as pores of the GACs. Despite the fact that BP is thicker than PHE, its adsorption on the GACs was still higher than that of PHE. This was attributed to its nonplanar configuration, allowing the two aromatic rings of BP to adjust their relative position by rotating around the C–C (σ bond connecting them) [Guo et al., 2008]. In other words, the flexible nonplanar BP can change its molecular configuration and has more access to the small pores than the planar PHE molecule with a rigid structure. Overall, both BP and PHE adsorption are more sensitive to the pore geometry of the carbons than BNZ because their molecular sizes are larger and they have less access into the small pores.

To further investigate hydrophobic interactions, BP and 2HB adsorptions on the ACFs were compared (Figures 5.17 and 5.18). BP and 2HB have very similar molecular sizes but significantly different solubilities (Table 4.2). It was observed that 2HB had lower adsorption affinities than BP at the same concentration levels for each type of carbon. This is due to differences in the solubilities of these SOCs since they are very similar in molecular size and configuration. The substitution of a hydroxyl group in 2HB at an *ortho* position is the only difference between their molecular skeletons. This hydroxyl group in 2HB provides increased interactions of the compound with water via hydrogen-bond formation and increased water solubility and that, in turn, decreased the adsorption capacity. In other words, 2HB adsorption requires the disruption of relatively strong solute/solvent interactions, and therefore, adsorption of 2HB is energetically less favorable than adsorption of BP, which has weaker solute/solvent interactions.

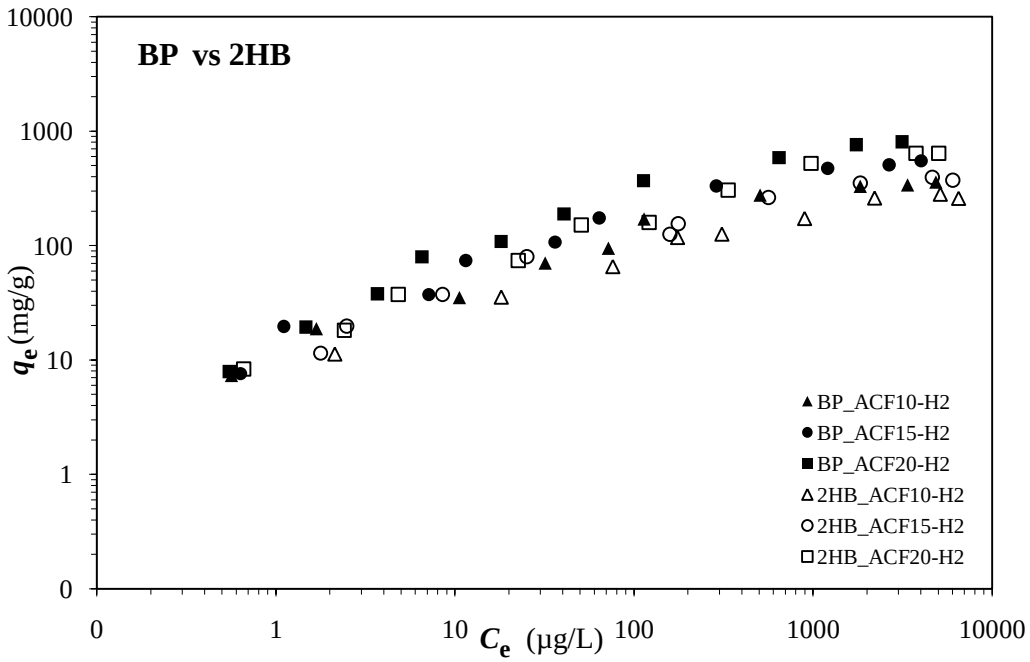

Figure 5.17 BP and 2HB adsorption isotherms on the heat-treated ACFs.

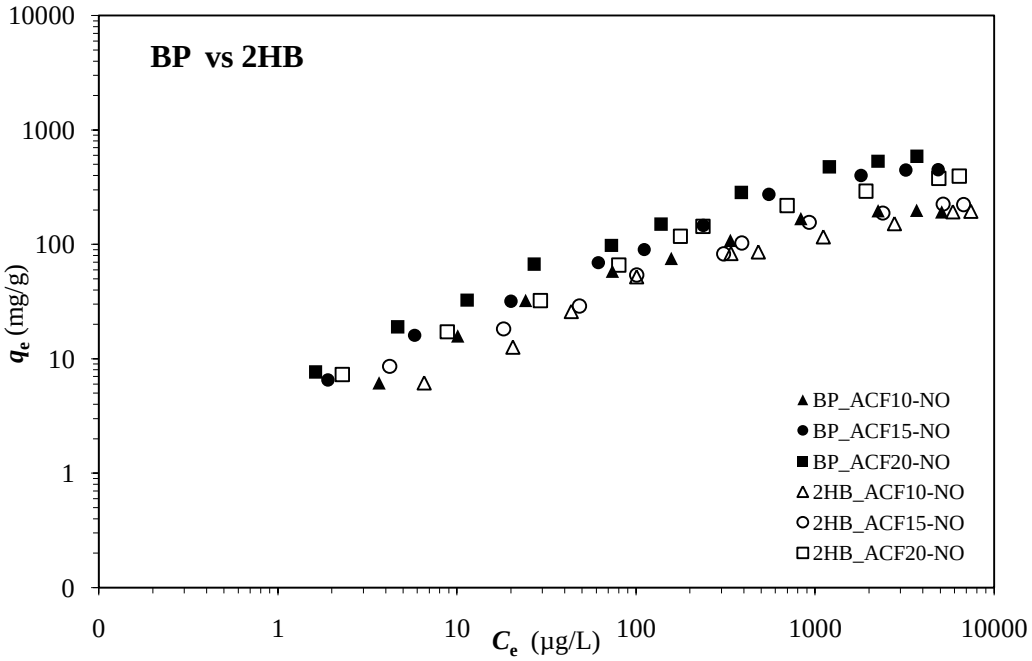

Figure 5.18 BP and 2HB adsorption isotherms on the oxidized ACFs.

In contrast to the mass-basis adsorption isotherms, the solubility-normalized isotherms of BP and 2HB showed a different trend (Figures 5.19 and 5.20). The adsorptions of 2HB were higher than those of BP for all six carbons probably due to the π-π electron-donor-acceptor (EDA) interactions. While the -OH group of 2HB extends the electron-donating ability, the oxygen groups on the ACFs, which are lower for heat-treated carbons and higher for the oxidized carbons, can serve as electron donor or acceptor and consequently contribute to the π-π EDA interactions. This results in an enhanced interaction between 2HB and the carbons. However, the lower K_F values of 2HB indicate that the π-π EDA interaction was not strong enough to compensate for the weak hydrophobic interactions between 2HB and ACFs due to the higher aqueous solubility of 2HB [Zhang et al, 2010].

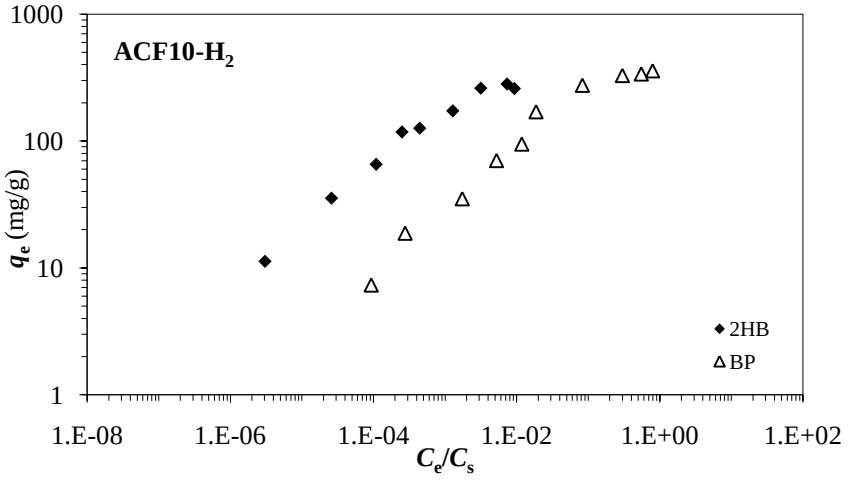

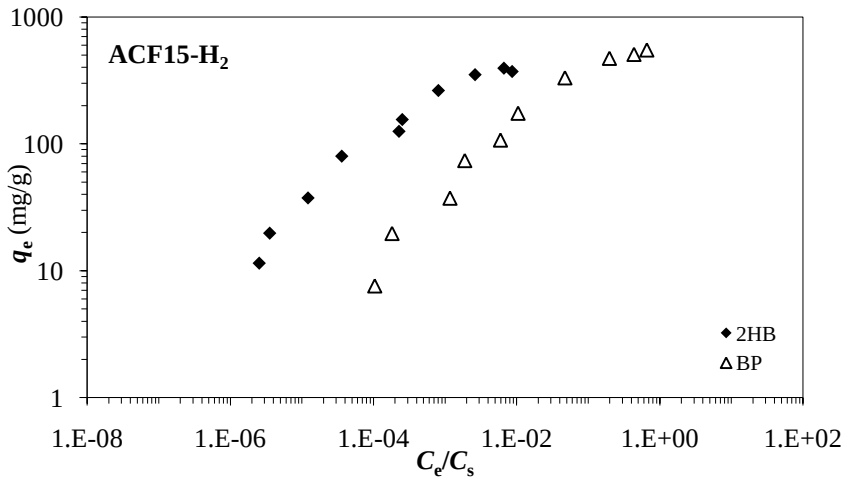

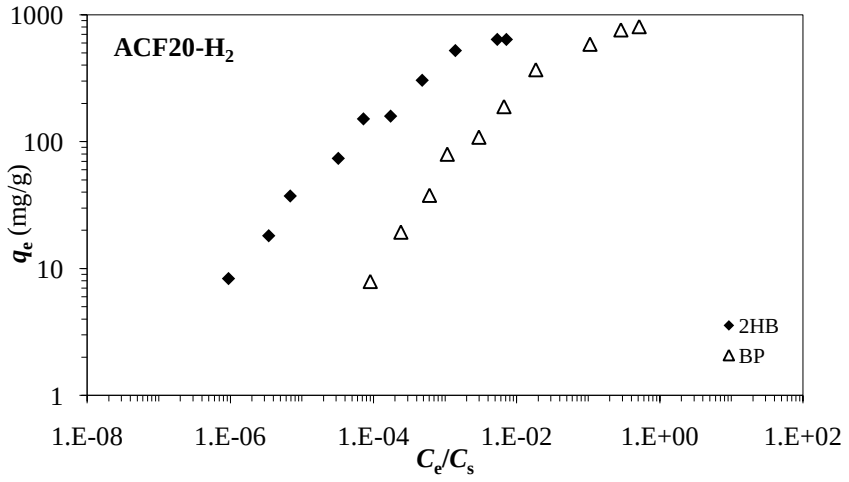

Figure 5.19 Comparison of the BP and 2HB solubility-normalized adsorption isotherms on the heat-treated ACFs.

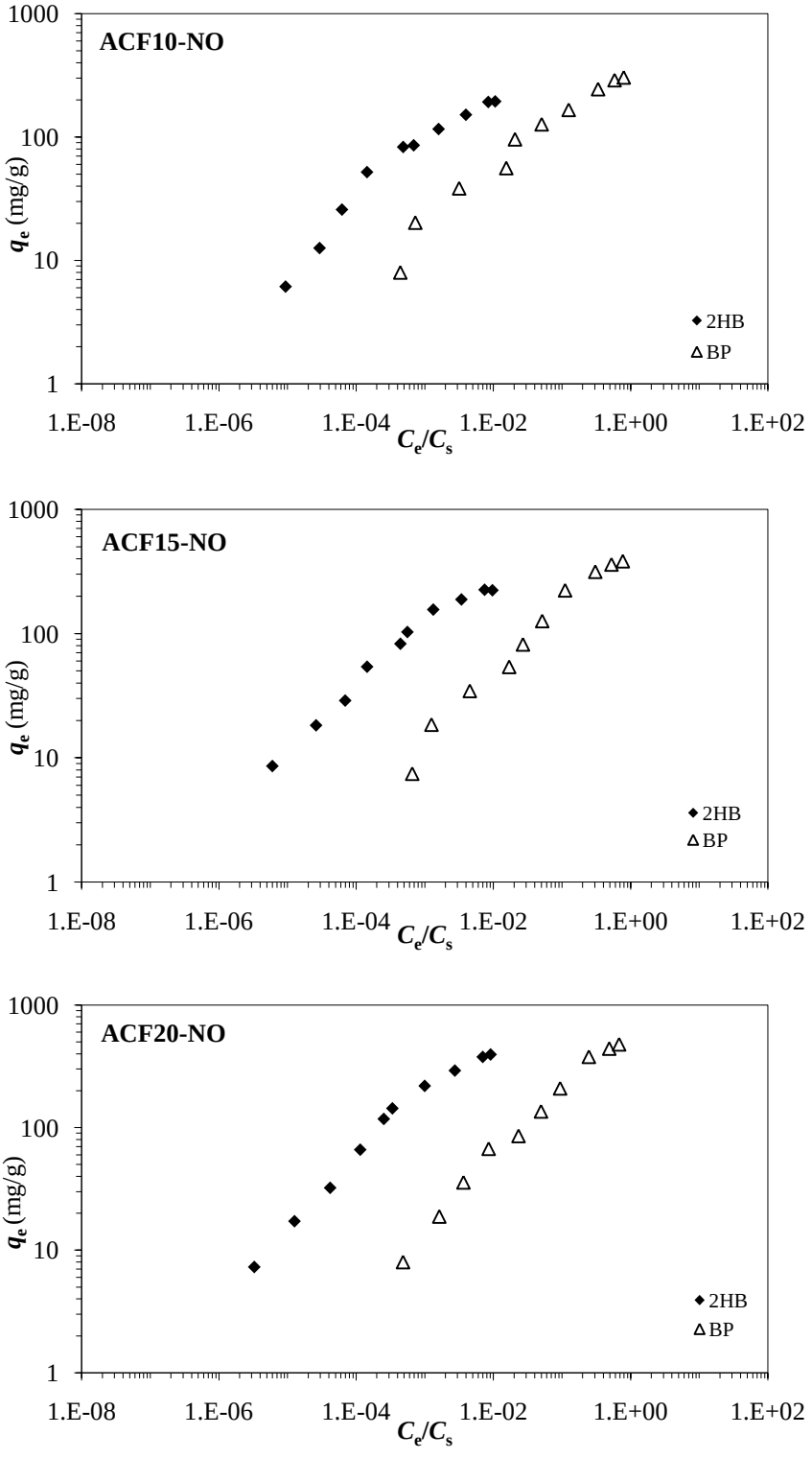

Figure 5.20 Comparison of the BP and 2HB solubility-normalized adsorption isotherms on the oxidized ACFs.

5.5 The Impact of the Carbon Surface Oxidation on SOC Adsorption

To examine the impact of the carbon surface chemistry and water-adsorbent interactions on SOC adsorption, BP and 2HB isotherms were conducted with the heat-treated and oxidized ACFs. Adsorption isotherms of BP and 2HB are illustrated in Figure 5.21 and Figure 5.22, respectively. Adsorption isotherms showed a curved relationship between q_e and C_e, which is possibly an indicator of two different adsorption regions: a continuous increase in adsorption was observed at low C_e values, and then adsorption reached the capacity of the carbons at high C_e values [Walters and Luthy, 1984]. The Freundlich isotherm parameters, expressed in two different units for comparison, are given in Table 5.5.

The results showed that both BP and 2HB adsorptions by the heat-treated ACFs were higher than those of the oxidized ACFs. Furthermore, regardless of the surface modification characteristics, adsorption increased with increasing level of activation (i.e., ACF20> ACF15>ACF10). This is expected since the specific surface areas are positively correlated with increasing level of activation.

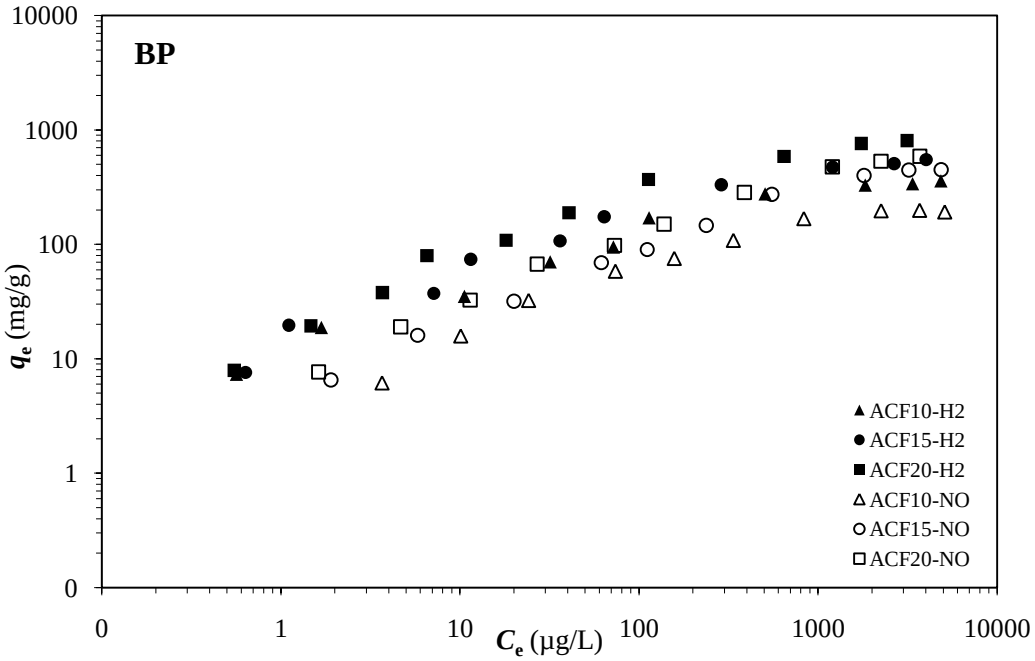

Figure 5.21 BP adsorption isotherms for heat-treated and oxidized ACFs.

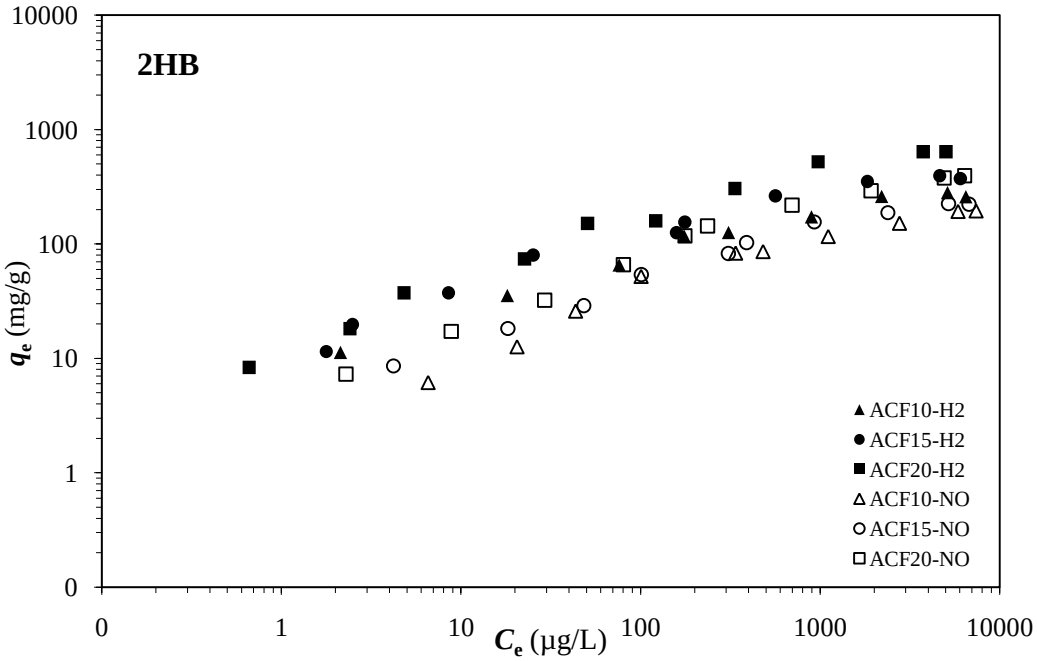

Figure 5.22 2HB adsorption isotherms for heat-treated and oxidized ACFs.

Table 5.5 Freundlich isotherm parameters of BP and 2HB.

SOC	Adsorbent	K_F[a] [(mg/g)/Ce^n]		n	r^2
		(μg/L)	(mg/L)		
BP	ACF10-H_2	13.99	262	0.42	0.954
	ACF15-H_2	17.02	421	0.46	0.949
	ACF20-H_2	19.45	711	0.52	0.946
	ACF10-NO	5.92	142	0.46	0.907
	ACF15-NO	6.12	273	0.55	0.979
	ACF20-NO	7.83	377	0.56	0.981
2HB	ACF10-H_2	11.18	173	0.40	0.964
	ACF15-H_2	14.35	254	0.42	0.954
	ACF20-H_2	14.84	383	0.47	0.958
	ACF10-NO	4.22	102	0.46	0.956
	ACF15-NO	4.92	120	0.46	0.963
	ACF20-NO	6.76	213	0.50	0.959

[a] Mass-basis adsorption affinity expressed in different units.

The heat-treated and oxidized counterparts of ACFs had very similar (i.e., within 10%) surface areas and pore volumes (Tables 5.1 and 5.2). Therefore, their physical structural parameters cannot explain their differences in adsorption behavior to BP and 2HB. The major differences between these two groups of ACFs were in their oxygen and nitrogen contents (Table 5.3), which were higher for the oxidized ACFs and lower for the heat-treated ACFs. Low oxygen and nitrogen contents provided basic hydrophobic surfaces with higher pH_{PZC} values, whereas high oxygen and nitrogen contents resulted in acidic hydrophilic surface character for the carbons with lower pH_{PZC} values. As previously stated, oxygen and nitrogen functional groups impair the adsorption of organic compounds since they can serve as hydrogen-bond donor and/or acceptor sites which

interact with water molecules more than they interact with organic compounds. The heat-treated carbons with their low oxygen and nitrogen contents were more hydrophobic. Consequently, their affinities for organic compounds were higher; and thus, they showed better adsorption potentials, as observed in previous studies [Kaneko et al., 1989; Li et al., 2002; Karanfil and Dastgheib, 2004; Cheng, 2006].

As displayed with the water vapor adsorption isotherms (Figure 5.3), the oxidized ACFs demonstrated higher affinities for water than the heat-treated ones at the low relative pressure range (below 0.4), which also supported the presence of the surface functional groups, and were related to the water cluster formation on the hydrophilic sites. Water clusters prevent organic compounds access to the basal planes of adsorbent and/or reduce the interaction energy between the compounds and the adsorbent surface, especially at low concentrations [Zhang et al., 2007]. In fact, both adsorption isotherms and Freundlich isotherm parameters well reflected the effects of functional groups and water cluster formation on the SOC adsorption. The isotherm differences between the oxidized and heat-treated ACFs were larger at low concentrations, whereas the isotherms converged at high concentrations. Furthermore, BP and 2HB uptakes were in the order of ACF20-H_2 > ACF15-H_2 > ACF10-H_2 > ACF20-NO > ACF15-NO > ACF10-NO at low concentrations, while isotherms showed different trends at higher concentrations. The three oxidized ACFs remained separated from each other regardless of the concentration level. In contrast, the value of the three heat-treated ACFs overlapped at the lowest concentrations, whereas the differences in uptake increased as concentration increased.

Oxygen and nitrogen containing groups reduced the adsorption capacities of ACFs to aromatic compounds, and surface chemistry played a key role in the adsorption.

To elucidate the effect of the adsorbent surface polarity, which was expressed by the sum of the oxygen and nitrogen contents, on the BP and 2HB adsorption, distribution coefficients (K_D) were calculated. In the case of linear adsorption, the accumulation of a compound by the sorbent is directly proportional to the concentration of the compound in the aqueous phase as described below:

$$K_D = q_e/C_e \tag{5.8}$$

Where, K_D is referred as the constant of proportionality as well as the distribution coefficient, and expressed in terms of volume per unit mass [Weber et al., 1991].

In the case of nonlinear adsorption, which can be described by the Freundlich model, at a given equilibrium concentration, K_D can be recalculated by employing the following equation:

$$K_D = K_F * (C_e)^{n-1} \tag{5.9}$$

The K_D values at two different equilibrium concentrations, 10 µg/L and 4 mg/L, were plotted against the surface area normalized oxygen and nitrogen contents [(O+N)/S_{BET}] of the adsorbents, and are illustrated in Figures 5.23 and 5.24. Surface area normalization was considered since each carbon had different surface areas with different O+N contents. As displayed in Figures, regardless of the concentration level, K_D values decreased with increasing (O+N)/S_{BET} ratios, indicating that a negative relationship existed between the BP/2HB distribution coefficients and the polarity of the adsorbents.

The results confirmed the negative impact of the surface polarity and water cluster formation on the SOC adsorption.

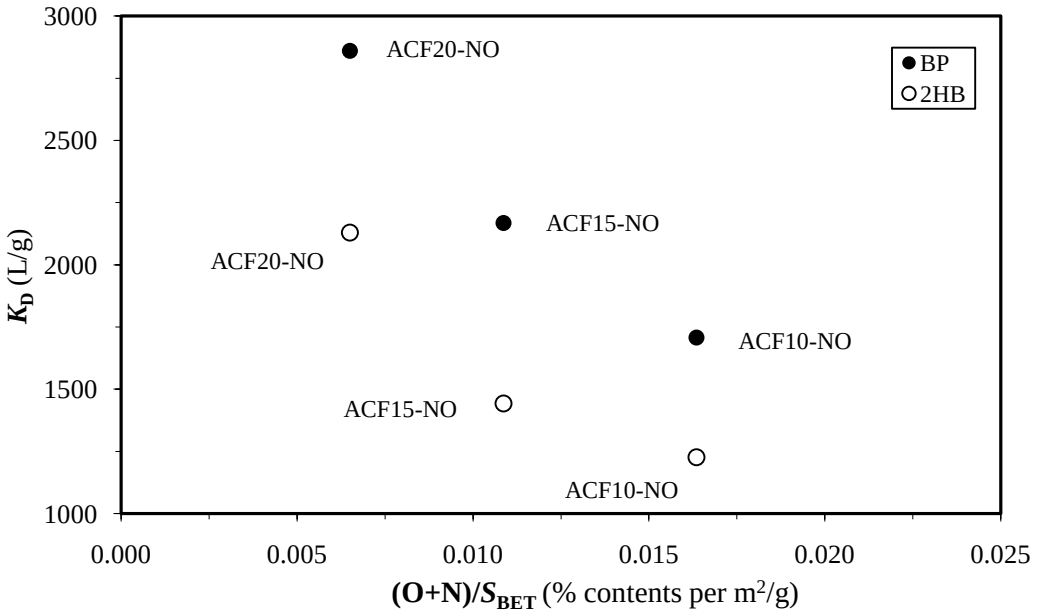

Figure 5.23 Relationships between distribution coefficients of the adsorbates and surface area normalized O+N contents of the adsorbents at C_e = 10 μg/L.

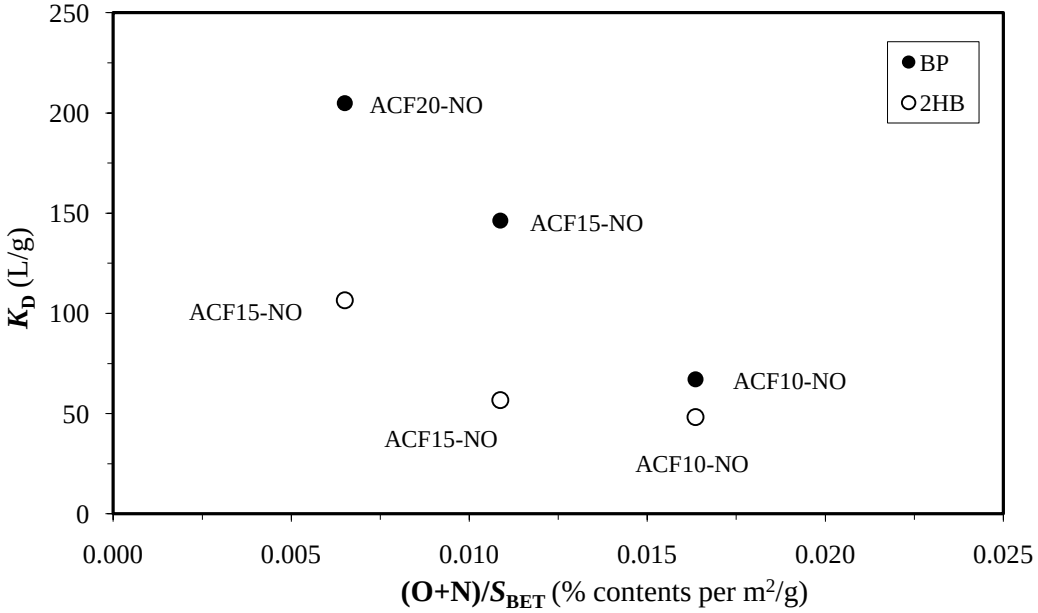

Figure 5.24 Relationships between distribution coefficients of the adsorbates and surface area normalized O+N contents of the adsorbents at C_e = 4 mg/L.

CHAPTER SIX

CONCLUSIONS AND RECOMMENDATIONS

The major conclusions obtained from this study are summarized below;

Objective 1: To examine the role of carbonaceous adsorbent physical characteristics (i.e., surface area, pore size distribution, precursor) on SOC adsorption.

- Activated carbon fibers (ACFs) exhibited higher adsorption capacities for the selected synthetic organic compounds (SOCs) than those of granular activated carbons (GACs) due to the higher specific surface areas and microporous structures of the ACFs. In addition, adsorption capacities increased with increasing activation level of the ACFs. Among the GACs, the coconut-based carbon demonstrated higher solubility- and surface area-normalized adsorption capacities than the coal-based carbons.
- Depending on the molecular dimensions of a compound, there was a specific optimum pore size region for each SOC. Both pore size distribution (PSD) and pore volume of pores less than 1 nm was the dominant adsorption site for benzene (BNZ), whereas pores 1 - 2 nm were important for the adsorption of biphenyl (BP) and phenanthrene (PHE).
- While adsorption of BNZ correlated with both surface areas and pore volumes, adsorption of BP and PHE was only related to the Brunauer-Emmett-Teller (BET) surface areas of the adsorbents. These relationships showed that there was no

restriction for BNZ molecules to access the pores because of its small size; however, size exclusion effects were observed for BP and PHE adsorption.

Objective 2: **To investigate the role of SOC characteristics (structure, dimension and configuration) on adsorption by ACs.**

- The adsorption uptake increased with decreasing molecular dimension of each compound and followed the order of BNZ > BP > PHE for the six heat-treated carbons.
- The importance of the molecular configuration was proved by comparing the adsorptions of BP and PHE. Adsorption capacities of BP were approximately two times higher than those of PHE for the six carbons. The flexible nonplanar BP could change its molecular configuration, and thus, had more access into the small pores than the planar PHE molecule with a rigid structure.
- BP had higher adsorption capacities than 2-hydroxybiphenyl (2HB) at the same concentration levels according to the mass-basis isotherms. The reason was attributed to the quite different solubilities of these SOCs since they were very similar in molecular size and configuration.
- According to the solubility normalized isotherms, 2HB showed higher uptakes than BP due to the π-π electron-donor-acceptor interactions, which resulted from the substitution of a hydroxyl group in the 2HB. However, this interaction was not strong enough to compensate for the weak hydrophobic interactions between 2HB and ACFs because of the higher aqueous solubility of 2HB.

Objective 3: To investigate the impact of the carbonaceous adsorbent surface oxidation (i.e., oxidized vs. heat-treated ACs) on SOC adsorption.

- The heat-treated ACFs had higher adsorption capacities than the oxidized ACFs, indicating that the oxygen and nitrogen containing groups reduced the adsorption capacities of ACFs to the selected SOCs. In other words, hydrophobic carbons were more effective for the removal of the both hydrophobic and hydrophilic compounds from aqueous solution.
- Regardless of the surface modification characteristics of the ACFs, adsorption increased with increasing level of activation. This was expected since the specific surface areas were positively correlated with the activation level.
- Oxygen and nitrogen containing groups reduced the adsorption capacities of ACFs to aromatic compounds, and surface chemistry played a key role in the adsorption.

Recommendations

Based on the results obtained in this study, the following recommendations are provided for applications and future research.

- For practical applications, it is important to consider the molecular dimensions of SOCs and the PSD of carbonaceous adsorbents in selecting adsorbents for treatment applications. The preference should be given to the adsorbents that have high pore volume in pores that are comparable to the molecular dimensions of the target SOCs to be removed from water or wastewater. It is also important to select

adsorbents with low surface polarity since it has been shown that water adsorption can hinder the adsorption of SOCs.

- Selecting additional organic compounds with different molecular sizes, solubilities, molecular configurations and different functional groups will be useful to further examine adsorption behavior of SOCs with different dimensions and structure.
- Conducting experiments with other well characterized adsorbents such as carbon nanotubes and graphite will be valuable to learn more about the role of carbon structure on SOC adsorption.
- It is important to investigate the adsorption behavior of these adsorbates and adsorbents in different background solutions, such as natural organic matter (NOM) or wastewater effluent organic matter in order to further extend the findings obtained in this study to practical applications.
- The results of this research are only based on the single-solute isotherm experiment. It is also important to understand the influence of both carbon pore structure and adsorbate molecular configuration on adsorption kinetics. Furthermore, these results could be further confirmed by performing rapid small scale column tests, simulating fixed-adsorbents in practical applications.

APPENDICES

APPENDIX A

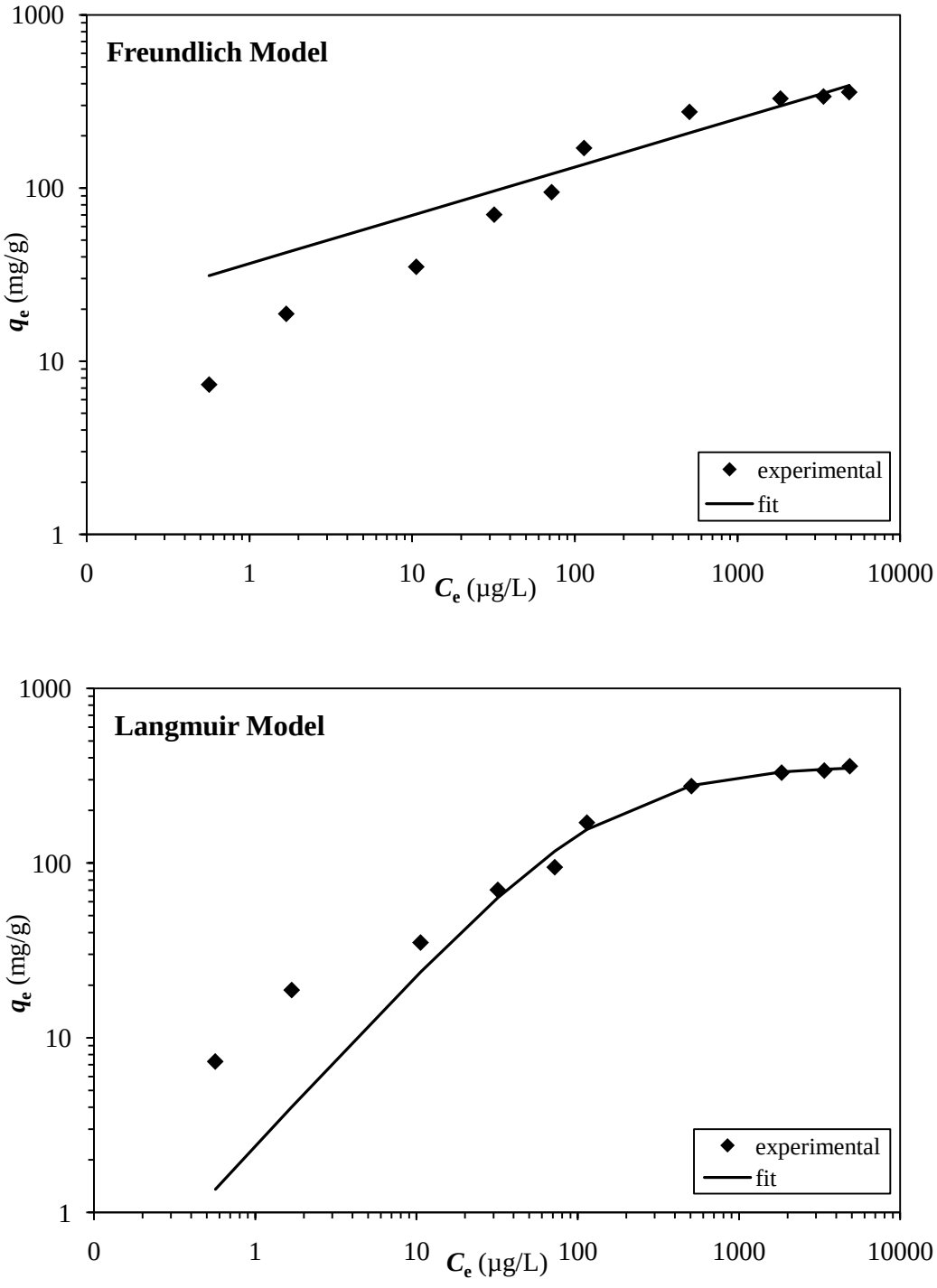

Figure A.1 Nonlinear Freundlich and Langmuir model isotherms of BP on ACF10-H_2.

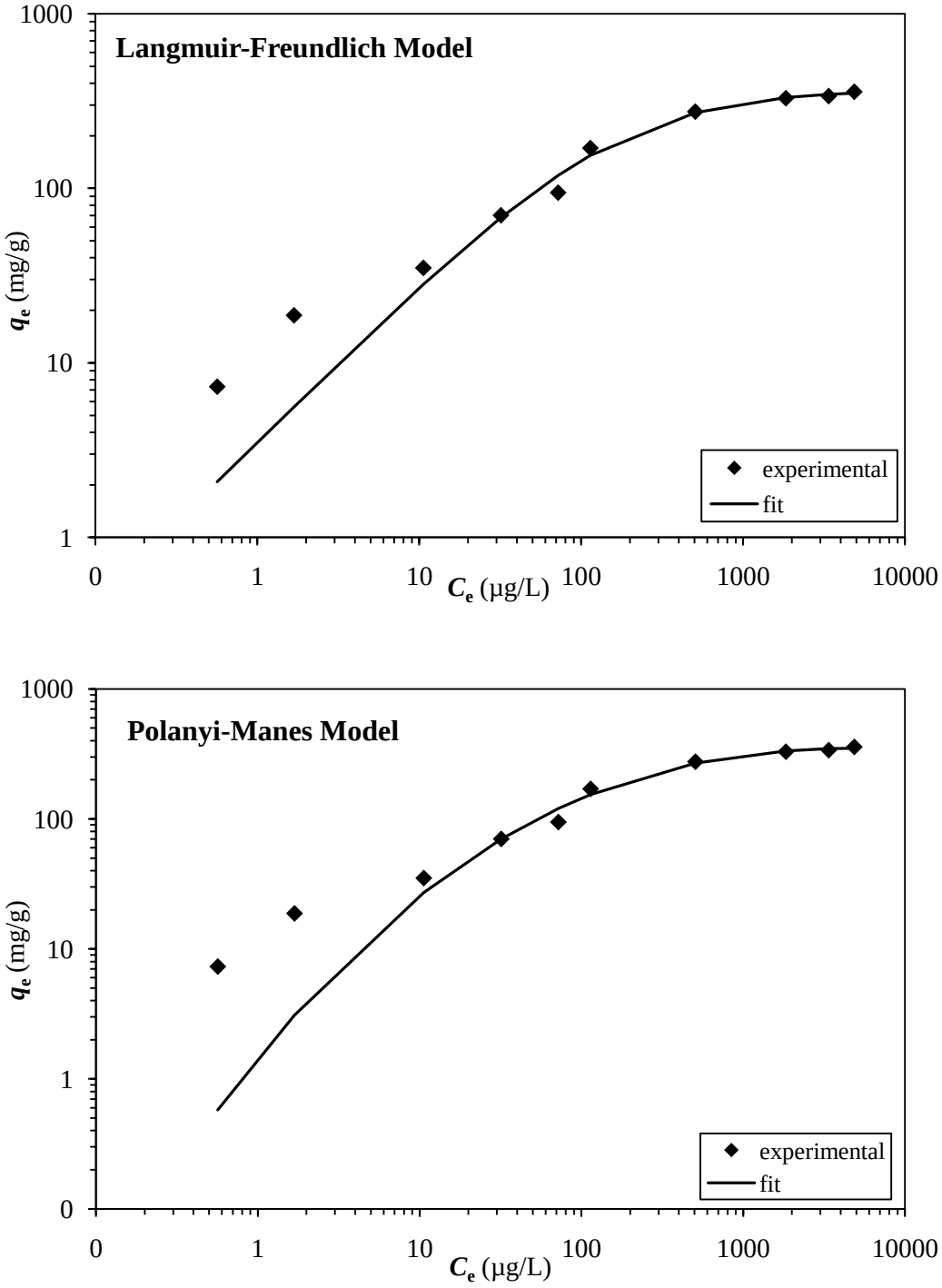

Figure A.2 Nonlinear Langmuir-Freundlich and Polanyi-Manes model isotherms of BP on ACF10-H_2.

Table A.1 Nonlinear model fits for adsorption of BNZ.

Adsorbents	Freundlich				Langmuir				Langmuir-Freundlich					Polanyi-Manes				
	K_F	n	r^2	RMSE	q_m	K_L	r^2	RMSE	q_m	K_S	n	r^2	RMSE	q_m	a	b	r^2	RMSE
ACF10-H_2	0.69	0.62	0.992	17.91	910	3.10^{-5}	0.978	30.43	3950	12.10^{-5}	0.67	0.991	20.71	77.10^4	-7.36	0.37	0.995	16.11
ACF15-H_2	1.28	0.57	0.992	18.59	845	4.10^{-5}	0.971	35.90	3980	22.10^{-5}	0.62	0.991	21.84	77.10^4	-6.90	0.34	0.995	15.26
ACF20-H_2	5.21	0.44	0.996	13.25	650	11.10^{-5}	0.965	39.05	4194	97.10^{-5}	0.47	0.996	14.15	77.10^4	-5.97	0.28	0.991	21.77
OLC-H_2	1.73	0.51	0.997	23.36	513	7.10^{-5}	0.971	26.23	4133	34.10^{-5}	0.54	0.978	24.57	77.10^4	-6.59	0.30	0.969	28.86
F400-H_2	1.93	0.48	0.992	10.60	398	8.10^{-5}	0.971	20.86	4139	39.10^{-5}	0.50	0.993	11.19	77.10^4	-6.44	0.28	0.986	15.39
HD4000-H_2	0.39	0.61	0.987	12.51	464	3.10^{-5}	0.973	17.98	4079	8.10^{-5}	0.64	0.986	14.57	77.10^4	-7.47	0.34	0.987	13.36

K_F [(mg/g)/(μg/L)^n]: adsorption affinity coefficient; n: nonlinear index; r^2: coefficient of determination; RMSE: residual root mean square error; q_m (mg/g): maximum adsorption capacity; K_L (L/μg): adsorption affinity coefficient; K_S [(L/μg)^n]: adsorption affinity coefficient; a and b: fitting parameters; underlined numbers represent the unreasonable values of the models.

Table A.2 Nonlinear model fits for adsorption of BP.

Adsorbents	Freundlich				Langmuir				Langmuir-Freundlich					Polanyi-Manes				
	K_F	n	r^2	RMSE	q_m	K_L	r^2	RMSE	q_m	K_S	n	r^2	RMSE	q_m	a	b	r^2	RMSE
ACF10-H_2	36.60	0.28	0.936	38.18	359	67.10^{-4}	0.993	12.67	367	96.10^{-4}	0.91	0.993	13.11	349	-298.8	2.43	0.992	14.59
ACF15-H_2	46.08	0.31	0.961	45.29	544	66.10^{-4}	0.992	20.42	607	179.10^{-4}	0.74	0.998	11.16	544	-100.7	2.01	0.997	12.78
ACF20-H_2	59.39	0.34	0.968	59.54	805	71.10^{-4}	0.989	35.36	955	203.10^{-4}	0.70	0.997	20.37	831	-77.4	1.90	0.997	20.09
ACF10-NO	19.26	0.29	0.911	23.72	211	45.10^{-4}	0.997	12.05	222	95.10^{-4}	0.84	0.980	11.65	204	-148.2	2.11	0.982	10.94
ACF15-NO	20.03	0.38	0.955	39.55	513	21.10^{-4}	0.995	12.82	512	21.10^{-4}	1.01	0.995	13.19	467	-198.4	2.06	0.995	14.19
ACF20-NO	20.22	0.42	0.969	40.04	669	18.10^{-4}	0.992	20.84	729	34.10^{-4}	0.87	0.993	20.09	614	-92.4	1.77	0.992	20.91
OLC-H_2	35.65	0.32	0.951	42.30	460	61.10^{-4}	0.993	16.00	492	125.10^{-4}	0.82	0.996	13.19	452	-153.2	2.15	0.995	14.71
F400-H_2	30.76	0.32	0.979	24.23	388	72.10^{-4}	0.943	40.35	754	281.10^{-4}	0.45	0.985	22.06	439	-17.5	1.29	0.984	22.50
HD4000-H_2	31.17	0.30	0.980	21.18	355	64.10^{-4}	0.994	35.61	602	328.10^{-4}	0.47	0.989	16.58	386	-19.9	1.37	0.989	16.83

K_F [(mg/g)/(μg/L)^n]: adsorption affinity coefficient; n: nonlinear index; r^2: coefficient of determination; RMSE: residual root mean square error; q_m (mg/g): maximum adsorption capacity; K_L (L/μg): adsorption affinity coefficient; K_S [(L/μg)^n]: adsorption affinity coefficient; a and b: fitting parameters; underlined numbers represent the unreasonable values of the models.

Table A.3 Nonlinear model fits for adsorption of PHE.

Adsorbents	Freundlich				Langmuir				Langmuir-Freundlich					Polanyi-Manes				
	K_F	n	r^2	RMSE	q_m	K_L	r^2	RMSE	q_m	K_S	n	r^2	RMSE	q_m	a	b	r^2	RMSE
ACF10-H_2	4.77	0.53	0.963	12.15	209	36.10^{-4}	0.964	11.87	294	64.10^{-4}	0.78	0.967	12.45	173	-34.1	1.26	0.966	12.77
ACF15-H_2	14.69	0.46	0.963	21.37	335	67.10^{-4}	0.989	11.81	333	65.10^{-4}	1.01	0.989	12.93	285	-165.3	1.85	0.987	13.74
ACF20-H_2	27.90	0.41	0.942	34.83	394	134.10^{-4}	0.980	20.54	380	108.10^{-4}	1.08	0.980	22.28	352	-598.9	2.41	0.980	22.66
OLC-H_2	1.26	0.82	0.940	22.10	608	9.10^{-4}	0.951	20.07	302	2.10^{-4}	1.52	0.959	18.98	255	-321.6	1.82	0.958	19.14
F400-H_2	2.68	0.65	0.991	7.65	343	17.10^{-4}	0.991	7.40	529	24.10^{-4}	0.82	0.993	7.20	225	-35.5	1.19	0.993	7.19
HD4000-H_2	4.39	0.59	0.980	12.38	321	26.10^{-4}	0.974	14.29	829	36.10^{-4}	0.69	0.981	13.24	256	-24.3	1.11	0.981	13.33

K_F [(mg/g)/(µg/L)^n]: adsorption affinity coefficient; n: nonlinear index; r^2: coefficient of determination; RMSE: residual root mean square error; q_m (mg/g): maximum adsorption capacity; K_L (L/µg): adsorption affinity coefficient; K_S [(L/µg)^n]: adsorption affinity coefficient; a and b: fitting parameters; underlined numbers represent the unreasonable values of the models.

Table A.4 Nonlinear model fits for adsorption of 2HB.

Adsorbents	Freundlich				Langmuir				Langmuir-Freundlich					Polanyi-Manes				
	K_F	n	r^2	RMSE	q_m	K_L	r^2	RMSE	q_m	K_S	n	r^2	RMSE	q_m	a	b	r^2	RMSE
ACF10-H_2	22.87	0.30	0.993	28.31	299	27.10^{-4}	0.970	19.11	327	80.10^{-4}	0.78	0.974	18.31	334	-689.7	3.73	0.970	19.54
ACF15-H_2	33.99	0.30	0.944	38.87	437	31.10^{-4}	0.976	25.37	480	102.10^{-4}	0.76	0.979	24.18	511	-294.8	3.31	0.975	26.88
ACF20-H_2	41.92	0.32	0.929	62.00	610	35.10^{-4}	0.970	40.72	646	75.10^{-4}	0.84	0.971	40.59	667	-1097.3	4.01	0.968	42.98
ACF10-NO	10.18	0.34	0.945	16.96	210	16.10^{-4}	0.951	15.99	270	93.10^{-4}	0.64	0.964	13.86	284	-100.1	2.56	0.963	14.05
ACF15-NO	12.33	0.34	0.956	16.82	234	19.10^{-4}	0.987	9.27	261	59.10^{-4}	0.78	0.991	7.78	274	-376.6	3.31	0.989	8.67
ACF20-NO	19.81	0.35	0.976	22.67	398	22.10^{-4}	0.986	17.24	495	96.10^{-4}	0.68	0.996	9.05	511	-180.9	2.92	0.997	8.23

K_F [(mg/g)/(µg/L)^n]: adsorption affinity coefficient; n: nonlinear index; r^2: coefficient of determination; RMSE: residual root mean square error; q_m (mg/g): maximum adsorption capacity; K_L (L/µg): adsorption affinity coefficient; K_S [(L/µg)^n]: adsorption affinity coefficient; a and b: fitting parameters; underlined numbers represent the unreasonable values of the models.

APPENDIX B

Table B.1 Freundlich coefficients for the adsorption isotherms of the SOCs along with the 95% confidence intervals and the standard errors.

SOC	Adsorbent	K_F[a] [(mg/g)/Ce^n]				*n*	
		(μg/L)	95% confidence intervals	(mg/L)	95% confidence intervals	(-)	95% confidence intervals
BNZ	ACF10-H_2	1.80 ± 0.08	2.88 - 1.13	65 ± 2.91	74 - 57	0.52 ± 0.03	0.57 - 0.47
	ACF15-H_2	2.91 ± 0.14	4.64 -1.82	80 ± 3.88	91 - 70	0.48 ± 0.03	0.53 - 0.43
	ACF20-H_2	3.11 ± 0.15	5.04 - 1.92	93 ± 4.39	106 - 81	0.49 ± 0.03	0.55 - 0.44
	OLC-H_2	1.39 ± 0.06	2.16 - 0.89	54 ± 2.43	61 - 47	0.53 ± 0.03	0.58 - 0.48
	F400-H_2	0.95 ± 0.05	1.64 - 0.55	43 ± 2.32	50 - 37	0.55 ± 0.03	0.61 - 0.49
	HD4000-H_2	0.32 ± 0.01	0.53 - 0.19	25 ± 1.01	29 - 22	0.63 ± 0.03	0.69 - 0.58
BP	ACF10-H_2	13.99 ± 1.36	19.49-10.04	262 ± 25.47	331- 208	0.42 ± 0.03	0.49 - 0.36
	ACF15-H_2	17.02 ± 1.75	24.34-11.90	421 ± 43.30	564 - 315	0.46 ± 0.04	0.54 - 0.39
	ACF20-H_2	19.45 ± 2.31	28.38-13.33	711 ± 84.57	1015 - 499	0.52 ± 0.04	0.60 - 0.44
	ACF10-NO	5.92 ± 0.45	8.40 - 4.18	142 ± 10.87	169 - 120	0.46 ± 0.03	0.52 - 0.40
	ACF15-NO	6.12 ± 0.29	8.27 - 4.53	273 ± 12.98	323 - 230	0.55 ± 0.03	0.60 - 0.50
	ACF20-NO	7.83 ± 0.34	9.27 - 6.61	377 ± 16.25	420 - 338	0.56 ± 0.02	0.59 - 0.53
	OLC-H_2	9.98 ± 1.37	17.71 - 5.62	344 ± 47.31	499 - 238	0.51 ± 0.06	0.62 - 0.40
	F400-H_2	12.87 ± 1.87	22.06 - 7.51	290 ± 42.24	419 - 201	0.45 ± 0.05	0.55 - 0.35
	HD4000-H_2	13.04 ± 1.79	21.97 - 7.74	263 ± 36.19	372 - 186	0.44 ± 0.05	0.53 - 0.34
PHE	ACF10-H_2	2.84 ± 0.20	4.76 - 1.70	197 ± 13.51	248 - 156	0.61 ± 0.05	0.71- 0.51
	ACF15-H_2	7.41 ± 0.52	11.93 - 4.61	404 ± 28.16	524 - 312	0.58 ± 0.05	0.68 - 0.48
	ACF20-H_2	13.65 ± 1.62	27.52 - 6.77	574 ± 68.06	913 - 360	0.54 ± 0.08	0.69 - 0.39
	OLC-H_2	0.67 ± 0.02	0.84 - 0.53	384 ± 11.74	431 - 342	0.92 ± 0.03	0.97 - 0.87
	F400-H_2	2.12 ± 0.10	3.10 - 1.45	239 ± 11.55	285 - 201	0.68 ± 0.04	0.76 - 0.61
	HD4000-H_2	1.86 ± 0.23	5.08 - 0.68	303 ± 36.76	483 - 190	0.74 ± 0.10	0.93 - 0.54
2HB	ACF10-H_2	11.18 ± 0.55	13.57 - 9.21	173 ± 8.57	192 - 157	0.40 ± 0.02	0.43 - 0.36
	ACF15-H_2	14.35 ± 0.88	20.11-10.24	254 ± 15.60	314 - 205	0.42 ± 0.03	0.48 - 0.36
	ACF20-H_2	14.84 ± 0.96	18.36-12.00	383 ± 24.74	445 - 329	0.47 ± 0.02	0.51 - 0.43
	ACF10-NO	4.22 ± 0.18	5.15 - 3.46	102 ± 4.36	111 - 91	0.46 ± 0.02	0.49 - 0.43
	ACF15-NO	4.92 ± 0.19	5.88 - 4.11	120 ± 4.58	129 - 111	0.46 ± 0.02	0.49 - 0.43
	ACF20-NO	6.76 ± 0.42	8.63 - 5.29	213 ± 13.11	242 - 187	0.50 ± 0.02	0.54 - 0.46

[a] Freundlich adsorption affinity expressed in different units.

APPENDIX C

Table C.1 Correlation results between structural parameters of the adsorbents and their adsorption capacities.

Structural Parameters	r^2		
	K_{FS} for BNZ	**K_{FS} for BP**	**K_{FS} for PHE**
S_{BET}	**0.801**[a]	**0.838**	**0.783**
S_{mic}	**0.750**	0.598	0.271
S (<1nm)	**0.895**	0.506	0.389
S (>1nm)	-1.746[b]	0.622	0.096
S (1-2 nm)	-1.388	0.781[c]	-0.022
V_{total}	-0.791	0.279	0.344
V_{mic}	**0.788**	0.657	0.362
V (<1nm)	**0.663**	0.224	0.051
V (>1nm)	-4.356	-0.634	-1.290
V (1-2 nm)	-1.544	0.754	-0.087

[a] Bold numbers represent the strong correlations, which were $r^2 > 0.65$; [b] Poor relationships were considered when $r^2 < 0.65$; [c] Underlined numbers were not taken into account because visual inspection of the data showed a good amount of scatter despite somewhat high r^2 values.

REFERENCES

Ania, C. O.; Cabal, B.; Parra, J. B.; Arenillas, A.; Arias, B. and Pis, J. J. (2008). Naphthalene adsorption on activated carbons using solvents of different polarity. *Adsorption*. 14(2-3):343-355.

Arafat, H. A.; Franz, M. and Pinto, N. G. (1999). Effect of salt on the mechanism of adsorption of aromatics on activated carbon. *Langmuir*. 15(18):5997-6003.

Bandosz, T. J. (2006). Desulfurization on activation carbons. In: *Activated Carbon Surfaces in Environmental Remediation*. Vol. 7. Bandosz, T.J. (Ed.). Elsevier, Academic Press, New York.

Brasquet, C. and Le Cloirec, P. (1997). Adsorption onto activated carbon fibers: Application to water and air treatments. *Carbon*. 35(9):1307-1313.

Brunauer, S.; Emmett, P.H. and Teller, E. (1938). Adsorption of gases in multimolecular layers. *The Journal of Physical Chemistry*. 60:309-319.

Carmo, A. M.; Hundal, L. S. and Thompson, M. L. (2000): Sorption of hydrophobic organic compounds by soil materials: Application of unit equivalent Freundlich coefficients. *Environmental Science and Technology*. 34(20):4363-4369.

Carrott, P. J. M.; Mourao, P. A. M.; Ribeiro Carrot, M. M. L. and Goncalves, E. M. (2005). Separating surface and solvent effects and the notion of critical adsorption energy in the adsorption of phenolic compounds by activated carbons. *Langmuir*. 21(25):11863-11869.

Carter, M. C. (1993). Analysis and modeling of the impacts of background organic matter on TCE adsorption by activated carbon. *Ph.D. Dissertation.* University of Michigan. Ann Arbor, MI.

Carter, M. C.; Kilduff, J. and Weber, Jr., W.J. (1995). Site energy distribution analysis of preloaded adsorbents. *Environmental Science and Technology*. 29(7):1773-1780.

Cheng, W. (2006). Removal of dissolved natural matter and control of disinfection by-products by modified activated carbons. *Ph.D. Dissertation*. Clemson University. Clemson, SC.

Chiou, C. C. T. and Manes, M. (1973). Application of the Polanyi adsorption potential theory to adsorption from solution on activated carbon. IV. Steric factors, as illustrated by the adsorption of planar and octahedral metal acetylacetonates. *The Journal of Physical Chemistry*. 77(6):809-813.

Chiou, C. C. T. and Manes, M. (1974). Application of the Polanyi adsorption potential theory to adsorption from solution on activated carbon. V. Adsorption from water of some solids and their melts, and a comparison of bulk and adsorbate melting points. *The Journal of Physical Chemistry*. 78(6):622-626.

Choma, J. and Jaroniec, M. (2006). Characterization of nanoporous carbons by using gas adsorption isotherms. In: *Activated Carbon Surfaces in Environmental Remediation*. Vol. 7. Bandosz, T.J. (Ed.). Elsevier, Academic Press, New York.

Considine, R.; Denoyel, R.; Pendleton, P.; Schumann, R. and Wong, S. H. (2001). The influence of surface chemistry on activated carbon adsorption of 2-methylisoborneol from aqueous solution. *Colloids and Surfaces*. 179(2-3):271-280.

Corapcioglu, M. O. and Huang, C. P. (1987). The surface acidity and characterization of some commercial activated carbons. *Carbon*. 25(25):569-579.

Cornelissen, G.; Elmquist, M.; Groth, I. and Gustafsson. O. (2004). Effect of sorbate planarity on environmental black carbon sorption. *Environmental Science and Technology*. 38(13):3574-3580.

Coughlin, R. W.; Ezra, F. S. and Tan, R. N. (1968). Influence of chemisorbed oxygen in adsorption onto carbon from aqueous solution. *Colloid and Interface Science*. 28(3-4):386-396.

CRC. (1990-1991). *Handbook of Chemistry and Phyhsics*. Lide, D. R. (Ed.). 71st ed. CRC Press.

Crittenden, J. C.; Trussell, R. R.; Hand, D. W.; Howe, K. J. and Tchobanoglous, G. (2005). *Water Treatment Principles and Design/MWH*. 2nd ed. John Wiley & Sons, Inc., New Jersey. p.1254

Dabrowski, A; Podkoscielny, P.; Hubicki, Z, and Barczak, M. (2005). Adsorption of phenolic compounds by activated carbon - A critical review. *Chemosphere*. 58(8): 1049-1070.

Daley, M. A.; Tandon, D.; Economy, J. and Hippo, E. J. (1996). Elucidating the porous structure of activated carbon fibers using direct and indirect methods. *Carbon*. 34(10):1191-1200.

Dastgheib, S. A. and Rockstraw, D. A. (2001). Pecan shell activated carbon: Synthesis, characterization, and application for the removal of copper from aqueous solution. *Carbon.* 39(12):1849-1855.

Dastgheib, S. A.; Karanfil, T. and Cheng, W. (2004). Tailoring activated carbons for enhanced removal of natural organic matter from natural waters. *Carbon*. 42(3): 547-557.

Davies, G. M. and Seaton, N. A. (1998). The effect of the choice of pore model on the characterization of the internal structure of microporous carbons using pore size distributions. *Carbon*. 36(10):1473-1490.

Derylo-Marczewska, A.; Goworek, J.; Swiatkovski, A. and Buczek, B. (2004) Influence of differences in porous structure within granules of activated carbon on adsorption of aromatics from aqueous solutions. *Carbon*. 42(2):301-306.

Dowaidar, A. M.; El-Shahawi, M.S. and Ashour I. (2007). Adsorption of polycyclic aromatic hydrocarbons onto activated carbon from non-aqueous media: 1. The influence of the organic solvent polarity. *Separation Science and Technology*. 42(16):3609-3622.

Dubinin, M. M. (1989). Fundamentals of the theory of adsorption in micropores of carbon adsorbents: Characteristics of their adsorption properties and microporous structures. *Carbon*. 27(3):457-467.

Economy's Group. (2003). Activated Carbon Fibers. Department of Material Science and Engineering. University of Illinois at Urbana-Champaign. Urbana, Illinois. http://economy.mse.uiuc.edu/ACF.htm. [Accessed March 2010].

Electronics Cooling. (2001). The Role of Natural Graphite in Electronic Cooling. http://www.electronics-cooling.com/articles/2001/2001_august_techbrief.php. [Accessed May 2009].

Franz, M.; Arafat, H. A. and Pinto, N. G. (2000). Effect of chemical surface heterogeneity on the adsorption mechanism of dissolved aromatics on activated carbon. *Carbon*. 38(13):1807-1819.

Freeman, J. J.; Gimblett, F. R. G. and Sing, K. S. W. (1989). Studies of activated charcoal cloth. 5. Modification of pore structure by impregnation with certain transition metal salts and oxo-complexes. *Carbon*. 27(1):85-93.

Foster, K. L. (1993). The role of micropore size and chemical nature of the pore surface on the adsorption properties of activated carbon fibers. *Ph.D. Dissertation*. University of Illinois at Urbana-Champaign. Urbana, Illinois.

Garcia, T.; Murillo, R.; Cazorla-Amoros, D.; Mastral, A. M. and Linares-Solano, A. (2004). Role of the activated carbon surface chemistry in the adsorption of phenanthrene. *Carbon*. 42(8-9):1683-1689.

Guo, Y.; Yadav, A. and Karanfil, T. (2007). Approaches to mitigate the impact of dissolved organic matter on the adsorption of synthetic organic contaminants by porous carbonaceous sorbents. *Environmental Science and Technology*. 41(22):7888-7894.

Guo, Y.; Kaplan, S. and Karanfil, T. (2008). The significance of physical factors on the adsorption of polyaromatic compounds by activated carbons. *Carbon*. 46(14): 1885-1891.

Hayes, J.S. (1985). Novoloid nonwovens. *Nonwoven Symposium*. TAPPI Press. pp. 257-263.

Inagaki, M. and Tascon, J. M. D. (1996). Pore formation and control in carbon materials. In: *Activated Carbon Surfaces in Environmental Remediation*. Vol. 7. Bandosz, T.J. (Ed.). Elsevier, Academic Press., New York.

Jonker, M. T. O. and Koelmans, A. A. (2001). Polyoxymethylene solid phase extraction as a partitioning method for hydrophobic organic chemicals in sediment and soot. *Environmental Science and Technology*. 35(18):3742-3748

Jonker, M. T. O. and Koelmans, A. A. (2002). Sorption of polycyclic aromatic hydrocarbons and polychlorinated biphenyls to soot and soot-like materials in the aqueous environment: Mechanistic considerations. *Environmental Science and Technology*. 36(17):3725-3734.

Jonker, M. T. O. and Smedes, F. (2000). Preferential sorption of planar contaminants in sediments from Lake Ketelmeer, The Netherlands. *Environmental Science and Technology*. 34(9):1620-1626.

Kaneko, Y.; Abe, M. and Ogino, K. (1989). Adsorption characteristics of organic compounds dissolved in water on surface-improved activated carbon fibers. *Colloids and Surfaces*. 37:211-222.

Kaneko, K.; Hanzawa, Y.; Iiyama, T. Kanda, T. and Suzuki, T. (1999). Cluster-mediated water adsorption on carbon nanopores. *Adsorption*. 5(1):7-13.

Kaneko, K.; Setoyama, N.; Suzuki, T. and Kuwabara, H. (1993). Ultramicroporosity of porous solids by He adsorption. *Proceedings of the Fourth International Conference on Fundamentals of Adsorption*, International Adsorption Society, Boston.

Karanfil, T. (2006). Activated carbon adsorption in drinking water treatment. In: *Activated Carbon Surfaces in Environmental Remediation*. Vol. 7. Bandosz, T.J. (Ed.). Elsevier, Academic Press, New York.

Karanfil, T. and Dastgheib, S.A. (2004). Trichloroethylene adsorption by fibrous and granular activated carbons: Aqueous phase, gas phase and water vapor adsorption studies. *Environmental Science and Technology*. 38(22):5834-5841.

Karanfil, T. and Kilduff, J. E. (1999). Role of granular activated carbon surface chemistry on the adsorption of organic compounds. 1. Priority pollutants. *Environmental Science and Technology*. 33(18):3217-3224.

Karanfil, T.; Dastgheib, S.A. and Mauldin D. (2006). Exploring molecular sieve capabilities of activated carbon fibers to reduce the impact of NOM preloading on trichloroethylene adsorption. *Environmental Science and Technology*. 40(4):1321-1327.

Kasaoka, S.; Sakata, Y.; Tanaka, E. and Naitoh, R. (1989). Preparation of activated fibrous carbon from phenolic fabric and its molecular sieve properties. *International Chemical Engineering.* 29(1):101-104.

Kyotani, T. (2000). Control of pore structure in carbon. *Carbon*. 38(2):269-286.

Lastoskie, C.; Gubbins, K. E. and Quirke, N. (1993a). Pore size distribution analysis of microporous carbons: A density functional theory approach. *The Journal of Physical Chemistry*. 97(18):4786-4796.

Lastoskie, C.; Gubbins, K. E. and Quirke, N. (1993b). Pore size heterogeneity and the carbon slit pore: A density functional theory approach. *Langmuir*. 9(10):2693-2702.

Le Cloirec, P.; Brasquet, C. and Subrenat, E. (1997). Adsorption onto fibrous activated carbon: Applications to water treatment. *Energy and Fuels*. 11(2):331-336.

Li, L.; Quinlivan, P. A. and Knappe, D. R. U. (2002). Effects of activated carbon surface chemistry and pore structure on the adsorption of organic contaminants from aqueous solution. *Carbon*. 40(12):2085-2100.

Manes, M. and Hofer, L. J. E. (1969). Application of the Polanyi adsorption potential theory to adsorption from solution on activated carbon. *The Journal of Physical Chemistry.* 73(3):584-590.

Mangun, C. L.; Benak, K. R.; Daley, M. A. and Economy, J. (1999). Oxidation of activated carbon fibers: Effect on pore size, surface chemistry, and adsorption properties. *Chemistry of Materials*. 11(12):3476-3483.

Mangun, C. L.; Benak, K. R.; Economy, J. and Foster, L. K. (2001). Surface chemistry, pore size and adsorption properties of activated carbon fibers and precursors treated with ammonia. *Carbon*. 39(12):1809-1820.

Menendez, J. A.; Phillips, J.; Xia, B. and Radovic, L. R. (1996). On the modification and characterization of chemical surface properties of activated carbon: In the search of carbons with stable basic properties. *Langmuir*. 12(18):4404-4410.

Menendez-Diaz, J. A. and Martin-Gullon, I. (2006). Types of carbon adsorbents and their production. In: *Activated Carbon Surfaces in Environmental Remediation*. Vol. 7. Bandosz, T.J. (Ed.). Elsevier, Academic Press, New York.

Moreno-Castilla, C. (2004). Adsorption of organic molecules from aqueous solutions on carbon materials. *Carbon*. 42(1):83-94.

Mowla, D.; Do, D. D. and Kaneko, K. (2003). Adsorption of water vapor on activated carbon: A brief overview. *Chemistry and Physics of Carbon*. 28:229-262.

Paredes, J. I.; Martinez-Alonso, A. and Tascon, J. M. D. (2003). Application of scanning tunneling and atomic force microscopies to the characterization of microporous and mesoporous materials. *Microporous and Mesoporous Materials*. 65(2-3):93-126.

Pelekani, C. and Snoeyink, V. L. (1999). Competitive adsorption in natural water: Role of activated carbon pore size. *Water Research*. 33(5):1209-1219.

Pelekani, C. and Snoeyink, V. L. (2000). Competitive adsorption between atrazine and methylene blue on activated carbon: The importance of pore size distribution. *Carbon*. 38(10):1423-1436.

Pignatello, J. J. and Xing, B. (1996). Mechanisms of slow sorption of organic chemicals to natural particles. *Environmental Science and Technology*. 30(1):1-11.

Pikaar, I.; Koelmans, A. A. and van Noort, P. C. M. (2006). Sorption of organic compounds to activated carbons. Evaluation of isotherm models. *Chemosphere*. 65(11):2343-2351.

Przepiorski, J. (2006). Activated carbon filters and their industrial applications. In: *Activated Carbon Surfaces in Environmental Remediation*. Vol. 7. Bandosz, T.J. (Ed.). Elsevier, Academic Press, New York.

Puri, B. R. (1970). Surface complexes on carbons. In: *Chemistry and Physics of Carbon*. Vol. 6. Walker, Jr. P. L. (Ed.). Marcel Dekker Inc., New York.

Radovic, L. R.; Silva, I. F.; Ume, J. I.; Menendez, J. A. Leon y Leon, C. A. and Scaroni, A. W. (1997). An experimental and theoretical study of the adsorption of aromatics possessing electron-withdrawing and electron-donating functional groups by chemically modified activated carbons. *Carbon*. 35(9):1339-1348.

Salame, I. I. and Bandosz, T. J. (1999) Experimental study of water adsorption on activated carbons. *Langmuir*. 15(2):587-593.

Shmidt, J. L.; Pimenov, A. V.; Lieberman, A. I. and Cheh, H. Y. (1997). Kinetics of adsorption with granular, powdered, and fibrous activated carbon. *Separation Science and Technology*. 32(13):2105-2114.

Sips, R. (1948). On the structure of a catalyst surface. *The Journal of Chemical Physics.* 16(5):490-495.

Snoeyink, V. L. and Summers, R. S. (1999). Chapter 13: Adsorption of organic compounds. In: *Water Quality and Treatment.* 5th ed. Letterman, R. D. (Ed.). McGraw-Hill, Inc., New York.

Snoeyink, V. L. and Weber, Jr., W. J. (1967). The surface chemistry of active carbon: Discussion of structure and surface functional groups. *Environmental Science and Technology*. 1(3):228-237.

Snoeyink, V. L.; Weber, W. J. and Mark, H. B. (1969). Sorption of phenol and nitrophenol by active carbon. *Environmental Science and Technology*. 3(10):918-926.

Stavropoulos, G. G.; Samaras, P. and Sakellaropoulos, G. P. (2007). Effect of activated carbons modification on porosity, surface structure and phenol adsorption. *Journal of Hazardous Materials*. 151(2-3):414-421.

Stoeckli, F.; Centeno, T. A.; Donnet, J. B.; Pusset, N. and Papirer, E. (1995). Characterization of industrial activated carbons by adsorption and immersion techniques and by STM. *Fuel*. 74(11):1582-1588.

Summers, R. S. and Roberts, P. V. (1988a). Activated carbon adsorption of humic substances: I. Heterodisperse mixtures and desorption. *Colloid and Interface Science*. 122(2):367-381.

Summers, R. S. and Roberts, P. V. (1988b). Activated carbon adsorption of humic substances: II. Size exclusion and electrostatic interactions. *Colloid and Interface Science*. 122(2):382-397.

USEPA Regulatory Agenda. (1995). Notice. Federal Register. 60:228:60610.

USEPA. (2009). Safe Drinking Water Act. http://www.epa.gov/safewater/sdwa/index.html. [Accessed March 2009].

Villacanas, F.; Pereira, M. F. R.; Orfao, J. J. M. and Figueiredo, J. L. (2006). Adsorption of simple aromatic compounds on activated carbons. *Colloid and Interface Science*. 293(1):128-136.

Walters, R. W. and Luthy, R. G. (1984). Equilibrium adsorption of polycyclic aromatic hydrocarbons from water onto activated carbon. *Environmental Science and Technology*. 18(6):395-403.

Webb, A. P. and Orr, C. (1997). Surface area and pore structure by gas adsorption. In: *Analytical Methods in Fine Particle Technology*. Camp, R.W.; Olivier, J. P. and Yunes, Y. S. (Eds.). Micromeritics Instrument Corporation, Norcross, GA.

Weber, Jr., W. J. (1972). *Physicochemical Processes for Water Quality Control*. Wiley-Interscience, New York..

Weber, Jr., W. J. and Van Vliet, B. M. (1980). Fundamental concepts for application of activated carbon in water and wastewater treatment. In: *Activated Carbon Adsorption of Organics from Aqueous Phase.* Vol. 1. Suffet, I. H. and McGuire, M. J. (Eds.). Ann Arbor Science Publishers, Inc., Ann Arbor, MI.

Weber, Jr., W. J.; McGinley, P. M. and Katz, L. E. (1991). Sorption phenomena in subsurface systems: Concepts, models and effects on contaminant fate and transport. *Water Research*. 25(5):499-528.

Wolff, W.F. (1959). A model of active carbon. *The Journal of Physical Chemistry*. 63:653-659.

Zhang, W.; Chang, Q. G.; Liu, W. D.; Li, B. J.; Jiang, W. X.; Fu, L. J. and Ying, W. C. (2007). Selecting activated carbon for water and wastewater treatability studies. *Environmental Progress*. 26(3):289-298.

Zhang, S.; Shao, T.; Kose, H. S. and Karanfil, T. (2010) Adsorption of aromatic compounds by carbonaceous adsorbents: A comparative study on granular activated carbon, activated carbon fiber and carbon nanotubes. *Environmental Science and Technology*. (In Press).

Zhang, S. (2010). Personal communication.